MicroRNA MiR-199a-5p regulates smooth muscle cell proliferation and morphology by targeting WNT2 signaling pathway

Author(s):
Gheinani, Ali Hashemi; Burkhard, Fiona C.; Rehrauer, Hubert; Aquino Fournier, Catharine; Monastyrskaya, Katia

Publication date:
2015-03

Permanent link:
https://doi.org/10.3929/ethz-b-000110812

Originally published in:
Journal of Biological Chemistry 290(11), https://doi.org/10.1074/jbc.M114.618694

THE JOURNAL OF BIOLOGICAL CHEMISTRY VOL. 290, NO. 11, pp. 7067–7086, March 13, 2015

MicroRNA MiR-199a-5p Regulates Smooth Muscle Cell Proliferation and Morphology by Targeting WNT2 Signaling Pathway*[S]

Received for publication, October 15, 2014, and in revised form, January 16, 2015 Published, JBC Papers in Press, January 16, 2015, DOI 10.1074/jbc.M114.618694

Ali Hashemi Gheinani[‡], Fiona C. Burkhard[§], Hubert Rehrauer[¶], Catharine Aquino Fournier[¶], and Katia Monastyrskaya[‡1]

From the [‡]Urology Research Laboratory, Department Clinical Research, University of Bern, 3010 Bern, Switzerland, [§]Department of Urology, University Hospital, 3010 Bern, Switzerland, and [¶]Functional Genomics Center Zurich, 8057 Zurich, Switzerland

Background: MicroRNA miR-199a-5p, implicated in cell motility and proliferation, is highly expressed in bladder smooth muscle.
Results: MiR-199a-5p regulates WNT, cytoskeleton, and cell cycle pathways in urothelial and smooth muscle cells and promotes myocardin-driven gene expression.
Conclusion: MiR-199a-5p acts via its target WNT2 to control smooth muscle proliferation and morphology.
Significance: MiR-199a-5p is a key modulator of smooth muscle hypertrophy, relevant for bladder organ remodeling.

MicroRNA miR-199a-5p impairs tight junction formation, leading to increased urothelial permeability in bladder pain syndrome. Now, using transcriptome analysis in urothelial TEU-2 cells, we implicate it in the regulation of cell cycle, cytoskeleton remodeling, TGF, and WNT signaling pathways. MiR-199a-5p is highly expressed in the smooth muscle layer of the bladder, and we altered its levels in bladder smooth muscle cells (SMCs) to validate the pathway analysis. Inhibition of miR-199a-5p with antimiR increased SMC proliferation, reduced cell size, and up-regulated miR-199a-5p targets, including WNT2. Overexpression of WNT2 protein or treating SMCs with recombinant WNT2 closely mimicked the miR-199a-5p inhibition, whereas down-regulation of WNT2 in antimiR-expressing SMCs with shRNA restored cell phenotype and proliferation rates. Overexpression of miR-199a-5p in the bladder SMCs significantly increased cell size and up-regulated SM22, SM α-actin, and SM myosin heavy chain mRNA and protein levels. These changes as well as increased expression of *ACTG2*, *TGFB1I1*, and *CDKN1A* were mediated by up-regulation of the smooth muscle-specific transcriptional activator myocardin at mRNA and protein levels. Myocardin-related transcription factor A downstream targets *Id3* and *MYL9* were also induced. Up-regulation of myocardin was accompanied by down-regulation of WNT-dependent inhibitory Krüppel-like transcription factor 4 in miR-199a-5p-overexpressing cells. In contrast, Krüppel-like transcription factor 4 was induced in antimiR-expressing cells following the activation of WNT2 signaling, leading to repression of myocardin-dependent genes. MiR-199a-5p plays a critical role in the WNT2-mediated regulation of proliferative and differentiation processes in the smooth muscle and may behave as a key modulator of smooth muscle hypertrophy, which is relevant for organ remodeling.

The main functions of the urinary bladder are urine storage and voiding. Normally, the bladder fills without distinct sensations and with no or only a marginal increase in intravesical pressure. However, in lower urinary tract dysfunction, this process is impaired by symptoms of urgency, frequency, and incomplete emptying. Lower urinary tract dysfunction causes profound changes in the gene expression profiles of both bladder urothelium and smooth muscle: in human bladder pain syndrome (BPS)[2] patients, the proteoglycan core proteins (1) and the tight junction proteins ZO-1, junctional adhesion molecule 1, and occludin (2) were down-regulated, implicating increased urothelial permeability. Bladder smooth muscle has a high level of plasticity and undergoes remodeling during lower urinary tract dysfunctions (3, 4). Benign prostatic hyperplasia can lead to bladder outlet obstruction accompanied by bladder hypertrophy (5). Bladder hypertrophy is characterized by significant changes in the expression profile of smooth muscle contractile and signaling proteins and modification of extracellular matrix proteins (6, 7).

MicroRNAs (miRNAs) are quickly gaining recognition for their role in many biological processes and disease states (8). MiRNAs are endogenous non-coding single-stranded RNAs of ~22 nucleotides that regulate gene expression by post-transcriptional mechanisms upon sequence-specific binding to their mRNA targets. MiRNAs are important modulators of

* This work was supported by Swiss National Science Foundation Grant 320030_135783 (to K. M.).
[S] This article contains supplemental files that include a list of primers and assays, mRNA-seq reads, read count information, selected genes for QPCR, and pathway analysis.
[1] To whom correspondence should be addressed: Urology Research Laboratory, Dept. of Clinical Research, University of Bern, Murtenstrasse 35, CH-3010 Bern, Switzerland. Tel.: 41-31-6328719; Fax: 41-31-6320551; E-mail: monastyk@dkf.unibe.ch.

[2] The abbreviations used are: BPS, bladder pain syndrome; RNA-seq, mRNA sequencing; QPCR, quantitative real time PCR; SM, smooth muscle; SMC, smooth muscle cell, WNT, wingless-type murine mammary tumor virus integration site family; MRTF, myocardin-related transcription factor; SRF, serum response factor; KLF4, Krüppel-like factor 4; miRNA, microRNA; ECM, extracellular matrix; RFP, red fluorescent protein; CTGF, connective tissue growth factor; MYL9, myosin regulatory light chain 9; Id3, inhibitor of DNA-binding protein 3; LSM, laser scanning module.

gene expression, and dysregulation of their synthesis contributes to many human diseases (9, 10). The first miRNA profiling in BPS has identified several miRNAs regulating the expression of signaling and adhesion molecules (2) that are relevant for the disease pathogenesis. The comparative analysis of the miRNA expression profiles in BPS, bladder cancer, and several inflammatory disorders showed that seven of 31 miRNAs altered in BPS had the same regulatory pattern in inflammatory bowel disease (11), which shares many features with BPS (12). Recently, the role of miRNAs in the bladder smooth muscle was investigated using an induced smooth muscle-specific Dicer knock-out, which caused a significant reduction of miRNA levels, including miR-145, miR-143, miR-22, miR-125b-5p, and miR-27a, leading to a disturbed micturition pattern *in vivo* (13). In a similar study, the loss of Dicer exacerbated cyclophosphamide-induced bladder overactivity in mice (14). MiR-29 is down-regulated in obstructed bladders, leading to increased ECM accumulation and fibrosis (15). Connexin 43 (GJA1), a major gap junction protein in bladder smooth muscle involved in regulation of contractility, has been shown to be repressed by the myocardin-responsive muscle-specific miR-1 with implications for postnatal bladder development and overactivity (16).

Previously, we identified miR-199a-5p as an important regulator of intercellular junctions (17). Upon overexpression in urothelial cells, it impairs correct tight junction formation and leads to increased permeability. MiR-199a-5p directly targets mRNAs encoding LIN7C, ARHGAP12, PALS1, RND1, and PVRL1 and attenuates their expression levels to a similar extent. The multiplicity of miR-199a-5p targets involved in the regulation of actin cytoskeleton and tight and adherens junction formation prompted us to carry out a comprehensive analysis of its effects on the transcriptome of transfected TEU-2 cells. Here, using next generation mRNA sequencing (RNA-seq) followed by GeneGo MetaCore pathway analysis, we identified the major signaling pathways regulated by this miRNA, including WNT signaling, cytoskeletal, and cell cycle pathways.

Our previous laser microdissection studies have shown that miR-199a-5p was predominantly expressed in bladder smooth muscle (17). We sought to elucidate its function in the bladder smooth muscle cells (SMCs) and investigated the effects of the alteration of its levels with antimiR- and miR-overexpressing lentiviral vectors on the smooth muscle morphology. We report that miR-199a-5p is a crucial regulator of the WNT signaling pathway in both TEU-2 and bladder SMCs, and it affects the proliferative and differentiation processes in the bladder smooth muscle.

EXPERIMENTAL PROCEDURES

Reagents and Antibodies

Monoclonal antibodies against smooth muscle (SM) α-actin (1A4) (A 2547), SM myosin heavy chain (M7786), and caldesmon (C21) (C0297) were from Sigma. Polyclonal anti-WNT2 antibody (ab27794) was from Abcam. Polyclonal anti-myocardin (sc-33766) and anti-inhibitor of DNA-binding protein 3 (Id3) (sc-490) and monoclonal anti- myocardin-related transcription factor (MRTF)-A (sc-398675) were from Santa Cruz Biotechnology, Inc. Alexa Fluor 488- and Cy3-labeled phalloidins were from Molecular Probes (Invitrogen). Restriction endonucleases, *Taq* polymerase, and T4 DNA ligase were purchased from New England Biolabs. Chemicals were from Sigma. Recombinant human DKK1 was from Sigma, and recombinant human WNT2 was from Abnova. The cell proliferation ELISA (BrdU) was from Roche Applied Science. G-LISA RhoA, Rac1, and Cdc42 kits were from Cytoskeleton, Inc.

Cell Culture and Transfection

The immortalized human urothelial cell line TEU-2 (18) was maintained in serum-free EpiLife Medium (Gibco®, Life Technologies) supplemented with human keratinocyte growth supplement and antibiotics (Gibco, Life Technologies). Differentiation of TEU-2 cells was achieved by addition of serum and Ca^{2+} as described previously (19). Pre-miR miRNA precursors for miR-199a-5p and a validated Cy3-labeled negative control were from Ambion (Applied Biosystems). The reverse transfections were done in 12-well plates with and without inserts (BD Biosciences, Falcon) using siPORT NeoFX Transfection Agent (Applied Biosystems). The transfected cells were incubated at 37 °C for 24, 48, or 72 h before mRNA isolation.

HEK293 cells were maintained in DMEM containing 2 mM glutamine (Biochrom), 100 units of penicillin/ml, 100 μg of streptomycin/ml, and 10% FCS (Gibco, Life Technologies). HEK293 cells were transiently transfected with reporter plasmids using Lipofectamine 2000 (Invitrogen) and assayed for luciferase activity 24 h post-transfection. Primary cultures of the human bladder SMCs were established following the papain-collagenase protocol as described previously (20). Cells were maintained in DMEM containing 2 mM glutamine, 100 units of penicillin/ml, 100 μg of streptomycin/ml, and 10% FCS. Cell passages between 1 and 6 were used. All the cell cultures were incubated at 37 °C at 85% humidity and 5% CO_2. Cell proliferation and metabolic activity were assessed using Alamar Blue reagent (Invitrogen) following the manufacturer's instructions.

Total RNA Isolation, Reverse Transcription, and Real Time PCR Analysis of mRNA and MiRNA Expression

Total RNA was isolated using the miRVana miRNA isolation kit (Ambion) as described previously (2, 21). The reverse transcription reactions were carried out using the High Capacity cDNA Reverse Transcription kit (Applied Biosystems) with random hexamer primers. The exon junction-spanning primers for SYBR Green quantitative real time PCR (QPCR) were designed by using PrimerBLAST software. Melting temperature, self-complementarity, and 3′ stability of primers were checked by Primer3Plus software, and primers were synthesized by Microsynth (Switzerland). TaqMan assays were from Applied Biosystems. Assay numbers and SYBR primer pairs used for QPCR are listed in supplemental file List of primers and assays.xlsx. Quantification of mature miR-199a-5p and endogenous control miRNA RNU48 was performed using TaqMan assays 000498 and 001006 with supplied assay-specific RT primers (Applied Biosystems). QPCR was carried out in triplicates using the 7900HT Fast Real-time PCR System (Applied Biosystems). The Ct values obtained after QPCR were normalized to the 18 S rRNA when performing TaqMan QPCR

and to the 28 S rRNA when performing SYBR Green QPCR. Ct values of miR-199a-5p TaqMan assay were normalized to RNU48. The end products of all PCRs were analyzed on a 4% low melting point agarose gel to validate the fragment size.

Firefly Luciferase Constructs and Luciferase Reporter Assays

A pmirGLO vector (Promega) containing the miR-199a-5p target sequence GAA CAG GTA GTC TGA ACA CTG GG was used as a positive control as described previously (17). To detect luciferase activity, the Dual-Luciferase Reporter Assay (Promega) was used, and the activity was normalized to *Renilla* luciferase expressed from the pmirGLO vector.

SDS-PAGE and Western Blotting Analysis

Unless otherwise stated, all procedures were performed at 4 °C or on ice. The cell lysates were analyzed by SDS-PAGE followed by Western blotting with specific antibodies. Image analysis to estimate the protein content of the individual bands following SDS-PAGE and Western blotting was performed using ImageJ software.

Phalloidin Staining and Live Cell Imaging

Bladder SMCs transduced with lentiviruses were grown on poly-L-lysine- and laminin-coated glass coverslips. For phalloidin staining, the cells were fixed with 4% paraformaldehyde, permeabilized in 0.05% Triton X-100 in PBS, and incubated with the Cy3- or Alexa Fluor 488-conjugated phalloidin. Inserts were mounted in PBS-gelvatol and examined under an Axiovert 200 M microscope with laser scanning module LSM 510 META (Zeiss). Live cell imaging was performed as described (22). Cells were observed under an Axiovert 200 M microscope with laser scanning module LSM 510 META using a ×20 or a ×40 oil immersion lens. Cell size (μm^2) was evaluated on captured images using Zeiss LSM software.

Lentivirus Production and Transduction of Bladder SM Cells

Total RNA was isolated from bladder SM cells, and cDNA was produced by reverse transcription with random hexamer primers as described above. Coding sequence of *WNT2* was PCR-amplified using forward primer 5′-AT AAA GCTAGC ATG AAC GCC CCT CTC GGTG-3′ and reverse primer 5′-ATA AA GGATCC TGT AGC GGT TGT CCA GTC AG-3′. Cloning NheI and BamHI sites are underlined. PCR fragments were inserted into pCDH-EF1-T2A-copGFP vector (System Biosciences, Mountain View, CA) to produce pCDH-WNT2 lentiviral vector. Lentiviral vectors overexpressing non-targeting scrambled miRNA, miR-199a-5p, and antimiR-199a-5p were as described previously (27). Lentiviruses expressing shRNA clones for WNT2 and a scrambled shRNA control, tagged with pmCherry, were from OmicsLink™ shRNA Expression Clones, GeneCopoeia (Rockville, MD) (catalog number HSH018529-1-LVRU6MP). The WNT2 target sequences of the shRNA clones were as follows: clone 1, TCC TGT GAT CCA AAG AAGA; clone 2, GGC TGC AGT GAT AAC ATTG; clone 3, TGT GGC CTT TAT CTC AACG; and clone 4, CCT GGA GAA GAA TGG CTTT. HEK293FT cells (System Biosciences) were plated at 50% confluence on 10-cm dishes and transfected with 12.5 μg of each of the pCDH-based lentiviral vectors, 7.5 μg of packaging pPAX2, and 4 μg of pMD2.G plasmids using Lipofectamine 2000 following the manufacturer's instructions. Supernatants collected 24 and 48 h after transfection were centrifuged at 4000 × *g*, filtered through a 0.45-μm-pore size cellulose acetate filter (Millipore, Billerica, MA), and mixed with PEG-it Virus Concentration Solution (System Biosciences) overnight at 4 °C. Viruses were precipitated at 1500 × *g* at 4 °C the next day and resuspended in PBS. The number of transducing infectious units of each stock was determined by infection of 293T cells followed by assessing the percentage of GFP-positive cells by fluorescence-activated cell sorting (FACS).

Subconfluent cultures of the primary bladder SMCs were transduced with recombinant lentiviral particles using 5×10^6 transducing infectious units/1×10^6 cells in the presence of 8 μg/ml Polybrene (Sigma). Typically, 70–95% cells were fluorescent reporter-positive 72 h post-transduction. Transduced cells were propagated and used in assays as described above.

Illumina RNA Sequencing

Library Preparation—The quality of the isolated RNA was determined with a Qubit® (1.0) fluorometer (Life Technologies) and a Bioanalyzer 2100 (Agilent, Waldbronn, Germany). Only those samples with a 260/280 nm ratio between 1.8 and 2.1 and a 28 S/18 S ratio within 1.5–2 were further processed. The TruSeq RNA Sample Prep kit v2 (Illumina, Inc.) was used in the succeeding steps. Briefly, total RNA samples (100–1000 ng) were poly(A)-enriched and then reverse transcribed into double-stranded cDNA. The cDNA samples were fragmented, end-repaired, and polyadenylated before ligation of TruSeq adapters containing the index for multiplexing. Fragments containing TruSeq adapters on both ends were selectively enriched with PCR. The quality and quantity of the enriched libraries were validated using a Qubit (1.0) fluorometer and the Caliper LabChip® GX (Caliper Life Sciences, Inc.). The product is a smear with an average fragment size of ~260 bp. The libraries were normalized to 10 nM in 10 mM Tris-Cl, pH 8.5 with 0.1% Tween 20.

Cluster Generation and Sequencing—The TruSeq PE Cluster kit v3-cBot-HS or TruSeq SR Cluster kit v3-cBot-HS (Illumina, Inc.) was used for cluster generation using 10 pM pooled normalized libraries on the cBot. Sequencing were performed on the Illumina HiSeq 2000 paired end at 2 × 101 bp or single end 100 bp using the TruSeq SBS kit v3-HS (Illumina, Inc.). Isoform expression was quantified using RSEM v1.1.15 (23). As a reference, we used the gene definitions from the University of California Santa Cruz for genome build hg19. RSEM was run with default parameters. Differential expression was computed with the Bioconductor package DESeq 1.4.1 (24). All hierarchical clusterings and the associated heat maps related to sequencing data were generated with the function heatmap2 in the R package gplots. For heat map visualization, the log expression values were used, and the values were normalized per gene by subtracting the mean.

Pathway Analysis

Transcripts with adjusted p value, false discovery rate q <0.05, and -fold change >1.5 were considered differentially

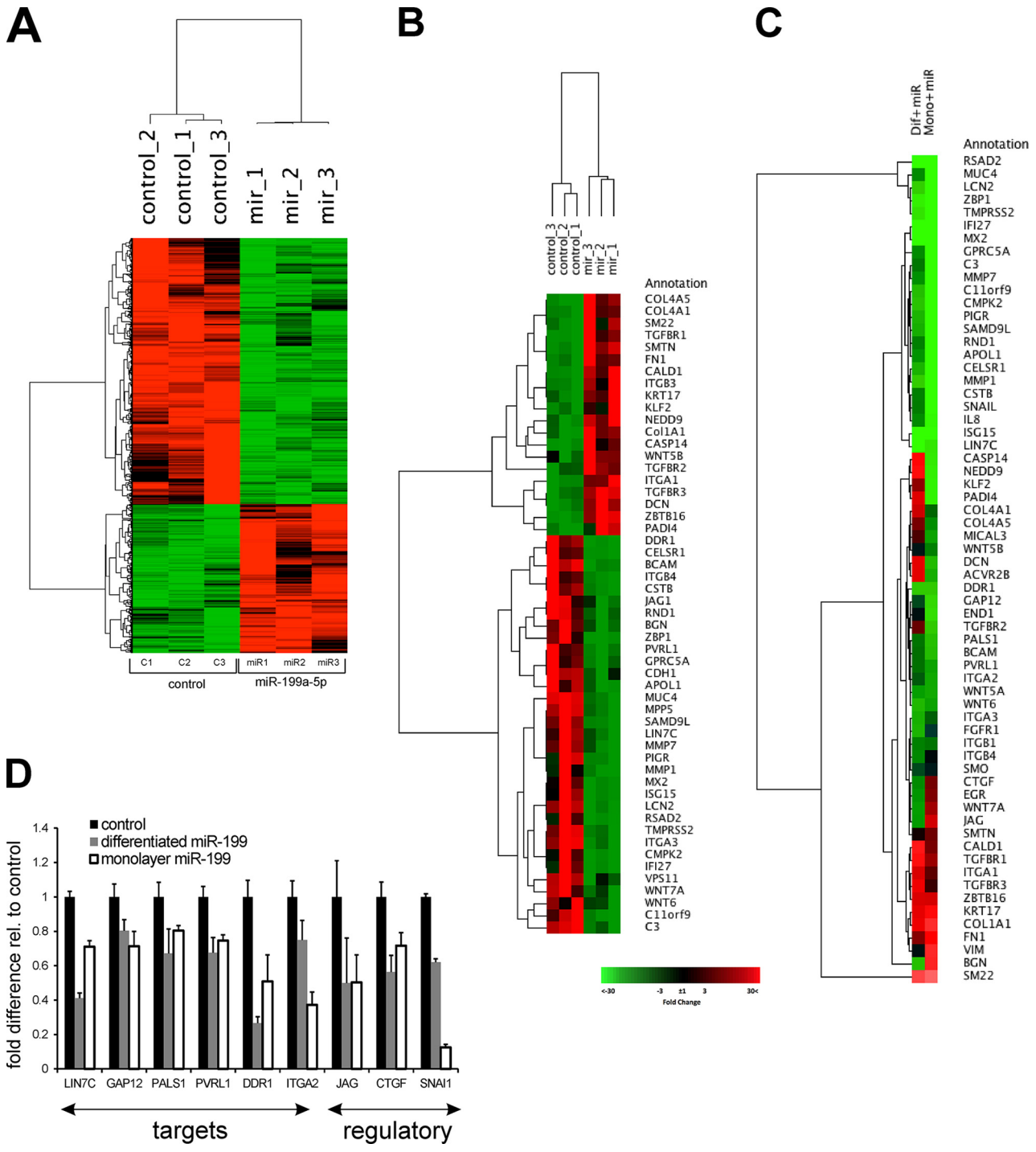

FIGURE 1. **Ectopic expression of miR-199a-5p in differentiated and non-differentiated TEU-2 cells causes profound changes in gene expression.** The TEU-2 cells transfected with pre-miR-199a-5p and negative control miR-Cy3 were grown on inserts in the presence of differentiation medium for 72 h ($n = 3$ samples per group). Total RNA was harvested, and total transcriptome analysis was performed following mRNA sequencing (next generation sequencing). *A*, heat map and hierarchical cluster analysis visualization of the $\log_2$ expression values obtained from 1646 genes. Values are normalized per gene. Color coding specifies expression of a given gene relative to the expression across the six samples. A dendrogram of clusters is shown on the *left* of the heat map. The expression level of a given gene is indicated by *red* (high) and *green* (low) in the heat map (significance threshold, 0.01; $\log_2$ ratio threshold, 0.5). The -fold changes between samples are variable, but there is a tight linear expression pattern for each gene, and the variability is due to selection of 1 − Correlation as a measure of distance. *B*, results for 53 genes included in further QPCR validation studies. *C*, effect of microRNA mir-199a-5p expression in differentiated *versus* non-differentiated TEU-2 cells. The heat map compares expression of 65 genes in TEU-2 cells in mir-199a-5p-transfected (*Mono*+*miR*) and mir-199a-5p-transfected differentiated (*Dif*+*miR*) TEU-2 cells. A panel of 65 genes was investigated by QPCR (primers and assays are shown in supplemental file List of primers and assays.xlsx) using cDNA from miR-overexpressing differentiated or non-differentiated (monolayer) TEU-2 cells. The *rows* correspond to different genes, and the *columns* represent the average of three experimental samples. The expression levels of genes in miR-199a-5p-transfected cells are shown as -fold changes relative to control non-targeting miR-Cy3 samples in monolayers and differentiated TEU-2 cells, respectively. The city block distance method was used to calculate the distance for clustering of the genes and samples. Genes of the known miR-199a-5p targets are down-regulated in both sample groups and clustered apart from those of involved in ECM and contraction. *D*, the mRNA levels were analyzed by QPCR, normalized to 28 S rRNA, and expressed as -fold difference relative (*rel.*) to the average values for miR-Cy3 cultures (either differentiated or monolayer). The graph shows an average of three experiments performed in triplicates ±S.E. (*error bars*). All differences were statistically significant ($p < 0.05$).

TABLE 1
Intersecting pathway maps regulated by miR-199a-5p

Rank	Common pathways	−log (*p* value)
1	Cytoskeleton remodeling via TGF, WNT	5.6
2	Signal transduction JNK pathway	4.1
3	Development WNT signaling pathway, part 2	3.6
4	Development regulation of epithelial-to-mesenchymal transition	3.2
5	Cytoskeleton remodeling	3.1
6	Development TGF-β receptor signaling	1.8
7	Cell cycle influence of Ras and Rho proteins on G_1/S transition	1.7
8	Cell adhesion chemokines and adhesion	1.7

expressed. Differentially expressed transcripts were then subjected to GeneGo MetaCore from Thomson Reuters (version 6.19, build 65960) to identify enrichment of pathways and processes using hypergeometric distributions to determine the most enriched gene sets with MetaCore variation of the Fisher's exact test and adjusting for multiple sample testing false discovery rate $q < 0.05$. Differentially affected pathways were defined based on standard deviation of the −log(p value), and then the resulting table of ontology was sorted in decreasing order of those standard deviation values.

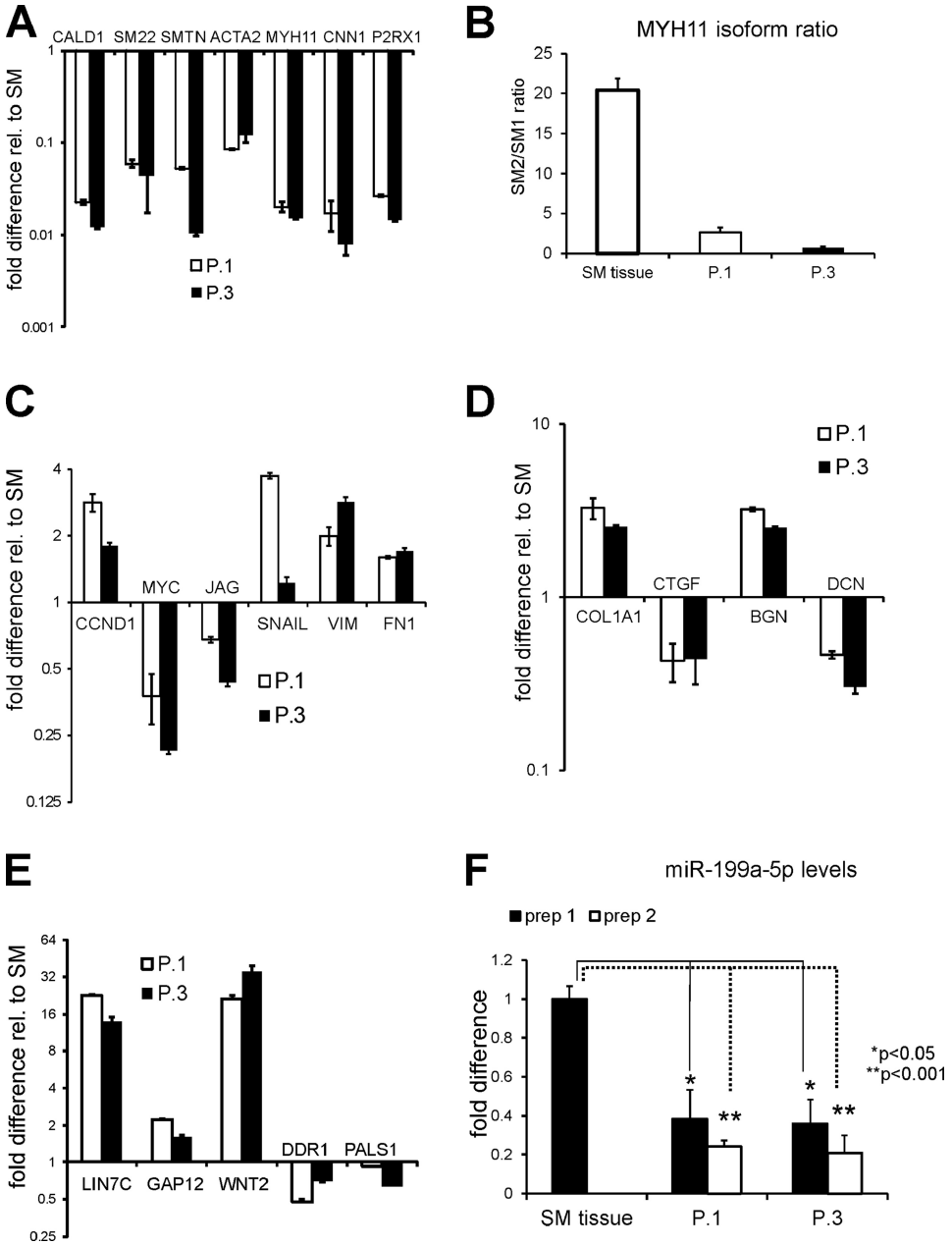

FIGURE 2. **Culturing of bladder smooth muscle cells induces gene expression changes.** Human bladder SM samples were used to raise primary cultures of SMCs. Cultures were passaged once (*P.1*) and three times (*P.3*), and the mRNA levels of selected genes were determined by QPCR and related to the levels in the original SM samples. The results were normalized to 28 S rRNA for SYBR Green primer pairs and 18 S rRNA for TaqMan assays and expressed relative (*rel.*) to the average values in the bladder SM samples. Each experiment was performed in triplicate. *A*, mRNA levels of smooth muscle-specific and contractile proteins; *B*, ratio of myosin heavy chain isoform SM2 to SM1; *C*, genes regulated by WNT; *D*, connective tissue growth factor and ECM proteins; *E*, validated miR-199a-5p targets; *F*, levels of mature miR-199a-5p were determined by QPCR, normalized to RNU48, and compared with the levels in SM tissue. The results of two independent SMC preparations (*prep 1* and *prep 2*) are shown. *A–F*, *error bars* represent S.E. Differences were statistically significant ($p < 0.05$).

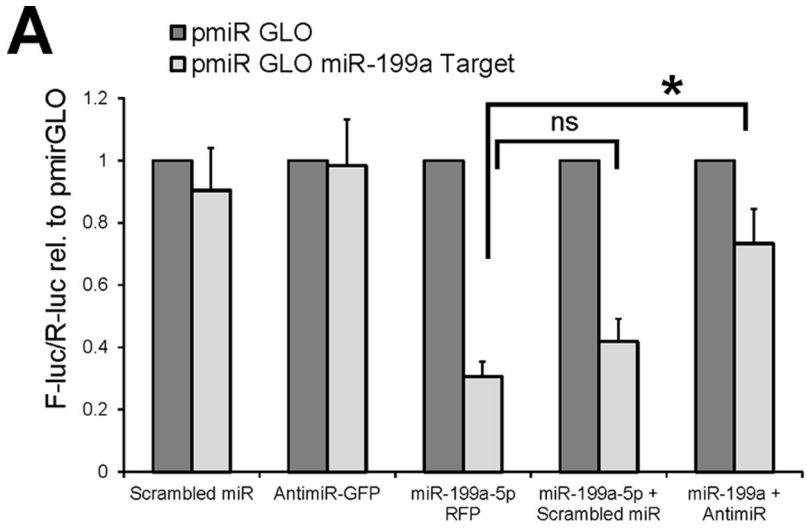
A
pmiR GLO
pmiR GLO miR-199a Target
F-luc/R-luc rel. to pmirGLO
1.2
1
0.8
0.6
0.4
0.2
0
ns
*
Scrambled miR
AntimiR-GFP
miR-199a-5p RFP
miR-199a-5p + Scrambled miR
miR-199a + AntimiR

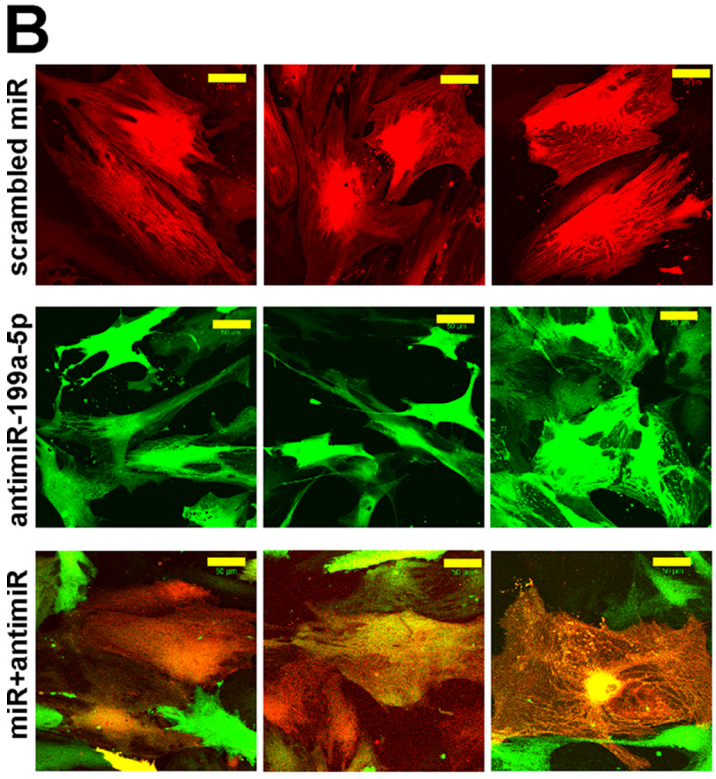
B
scrambled miR
antimiR-199a-5p
miR+antimiR

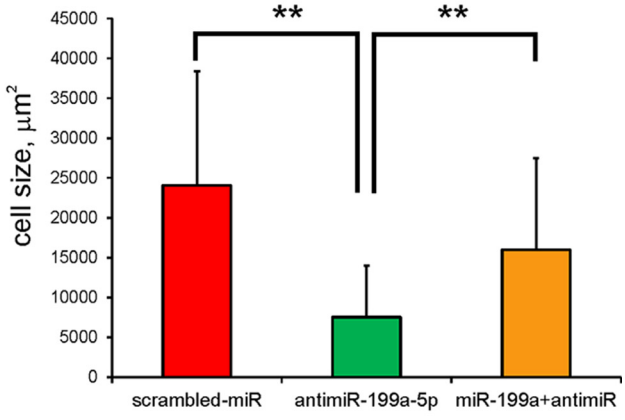
cell size, μm²
45000
40000
35000
30000
25000
20000
15000
10000
5000
0
**
**
scrambled-miR
antimiR-199a-5p
miR-199a+antimiR

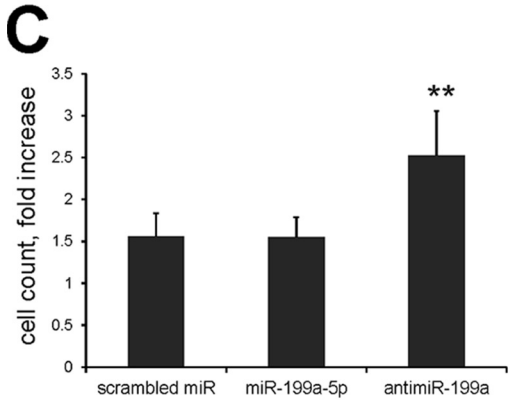
C
cell count, fold increase
3.5
3
2.5
2
1.5
1
0.5
0
**
scrambled miR
miR-199a-5p
antimiR-199a

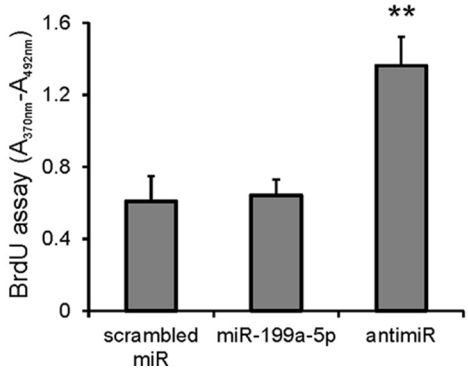
BrdU assay (A370nm-A492nm)
1.6
1.2
0.8
0.4
0
**
scrambled miR
miR-199a-5p
antimiR

Statistical and Data Analysis

Statistically significant differences were determined with a two-tailed Student's *t* test preceded by a Levene's test with α set to 0.05 for genes with a normal distribution. The results of cell assays were analyzed using one-way analysis of variance followed by Tukey's multiple comparison test or a two-tailed Student's *t* test preceded by a Levene's test. All studies were carried out with the SPSS program (version 20.0). All hierarchical clusterings and the associated heat maps related to QPCR data were generated with the function heatmap2 in the R package gplots. Unless otherwise stated, for heat map visualization, the -fold change values were used, the values were normalized per gene, and calculation of distance for clustering was done based on city block distance (Manhattan distance) and the average linkage method.

RESULTS

RNA-seq Transcriptome Profiling of the Differentiated TEU-2 Cells Overexpressing miR-199a-5p—Our recent study identified miR-199a-5p as an important regulator of intercellular junctions by targeting mRNAs encoding LIN7C, ARHGAP12, PALS1, RND1, and PVRL1 (17). Taking into account the multiplicity of miR-199a-5p-regulated target transcripts, we performed a comprehensive RNA-seq expression profiling of the differentiated TEU-2 cells transfected with miR-199a-5p precursor or scrambled non-targeting miRNA control. Total RNA sequencing resulted in 546 (paired end) million raw reads with an average of 91 million raw sequencing reads ranging from 68 to 106 million reads per sample. Approximately ~65% of the total reads were recorded with at least one reported alignment with reference genome hg19. Of these reads, an average of 43.7% corresponded to transcripts, 38.3% corresponded to mRNA exons, 5.5% corresponded to mRNA introns, 2.4% corresponded to mRNA promoter 2 kb, and 4.0% corresponded to mRNA downstream 2 kb (supplemental file Read count information.xlsx). About 30% of the mapped reads spanned two junctions, and 60% of the mapped reads spanned only one junction. The data are available at the European Nucleotide Archive (ENA) under accession number ERP006812.

Analysis of Genes with High Differential Expression in TEU-2 Cells Overexpressing MiR-199a-5p—Transcriptomes from differentiated TEU-2 cells transfected with miR-199a-5p were compared with those of the controls transfected with non-targeting miRNA to identify the effects of miR-199a-5p on gene expression. We observed differential expression of 1646 genes (3540 RefSeq ID) with 590 genes up-regulated and 1056 genes down-regulated in the miR-199a-5p-transfected TEU-2 cells (see supplemental file mRNA-seq reads.xlsx) (p value <0.05, false discovery rate <0.05, -fold change >1.5). A heat map of those 1646 significant differentially expressed genes is shown in Fig. 1*A*. Hierarchical cluster and heat map analyses consistently grouped the samples into two clusters: Cluster I, miR-199a-5p-transfected TEU-2 cells; Cluster II, non-targeting miR-Cy3-transfected controls.

The genes with q value <0.4, which were considered for further study, are listed in supplemental file Selected genes for QPCR.xlsx. These included the miR-199a-5p target genes identified previously (17) as well as genes expressed in TEU-2 cells and predicted to be targeted by miR-199a-5p using TargetScan, TarBase, miRecords, and Ingenuity® Knowledge Base databases. Other genes identified via the RNA-seq experiment were considered potentially novel miR-199a-5p-responsive genes. In addition to the down-regulated genes, mostly corresponding to the previously described or predicted miR-199a-5p targets such as *LIN7C*, *PALS1*, *DDR1*, and *JAG1*, we observed a number of mRNAs whose expression levels were significantly up-regulated in miR-overexpressing TEU-2 cells compared with the similarly differentiated controls (*COL4A1*, *COL1A1*, *FN1*, *SMTN*, *TGFBR1*, and *TGFBR3*) (Fig. 1*B*).

RNA-seq-based and in Silico Pathway Analysis of Differentiated TEU-2 Cells Overexpressing MiR-199a-5p—To identify the significant pathways represented by the 1645 genes with differential expression, a pathway analysis was conducted using GeneGo MetaCore from Thomson Reuters (version 6.19, build 65960). Among the top 50 pathway maps enriched in genes with differential expression, alteration of cell cycle; TGF, WNT, and cytoskeletal remodeling; and cell adhesion signaling pathways were mostly notable (supplemental file Pathway analysis.xlsx, sheet All regulated mRNA from mRNA-seq). To account for the possible differentiation-related effects, we performed two additional types of *in silico* pathway analysis, one using all validated and top score miR-199a-5p targets as defined by TargetScan, TarBase, miRecords, and Ingenuity Knowledge Base databases (supplemental file Pathway analysis.xlsx, sheet All miR-199a-5p targets), and the other using only the miR-199a-5p-targeted mRNAs expressed in TEU-2 (supplemental file Pathway analysis.xlsx, sheet Targets present in TEU2). Analysis of the intersection of the 50 top pathway maps revealed eight elements with cytoskeleton remodeling via TGF and WNT achieving the highest score (Table 1).

Verification of the MiR-199a-5p-responsive Genes by QPCR in Differentiated TEU-2 Cells and Monolayers—Tight junction assembly in TEU-2 cells is accompanied by the formation of a multilayered epithelium and differentiation-induced gene expression alterations (17). These changes overlap with miRNA-induced effects; therefore, we selected a subset of the top differentially expressed genes representing predicted miR-199a-5p targets, contractile and cytoskeletal proteins, and dif-

FIGURE 3. **Down-regulation of endogenous miR-199a-5p in bladder SMCs decreases cell size and increases proliferation.** *A*, antimiR-199a-5p effectively inhibits miR-199a-5p in the target binding luciferase assay. The perfectly complementary binding site for miR-199a-5p (target) was cloned into pmirGLO luciferase reporter vector and transfected into HEK293 cells stably transduced with lentiviruses expressing miR-199a-5p, antimiR-199a-5p, or scrambled miR control. *Renilla* luciferase activity expressed from the same vector was used for normalization, and the data were expressed relative (*rel.*) to the negative control pmirGLO vector. *Error bars* represent S.E. (*, $p < 0.05$). *B*, cultured primary human bladder SMCs (passage 1) were transduced with lentiviruses overexpressing scrambled miRNA control (RFP reporter) or antimiR-199a-5p (GFP reporter) and co-transduced with miR-199a-5p and antimiR-199a-5p. Cells were passaged once and examined live under an LSM microscope. *Scale bars*, 50 μm. Images of cells collected from random fields ($n = 100$ cells) were measured. The graph shows the average value in each sample ±S.D. (*error bars*) (**, $p < 0.005$). *C*, 3×10^4 cells were seeded per well, and cell count was analyzed 7 days postplating. Alternatively, cells were labeled with BrdU for 24 h, and a colorimetric proliferation BrdU ELISA was performed. Data are shown as -fold increase related to the initial plating density (*left* graph) or normalized optical density (*right* graph) ±S.D. (*error bars*) (**, $p < 0.005$).

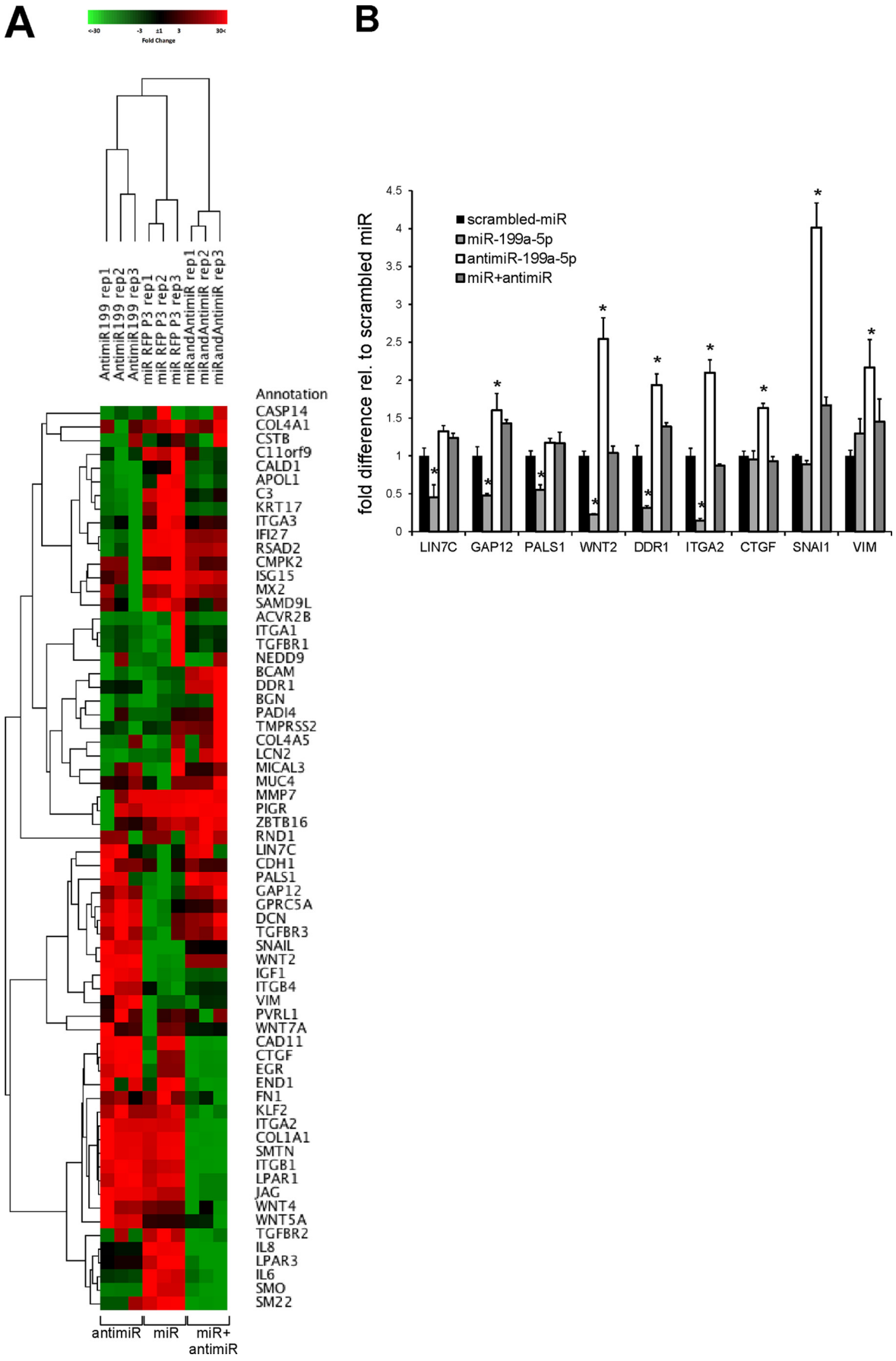
A
<-30
-3
±1
3
30<
Fold Change
AntimiR199 rep1
AntimiR199 rep2
AntimiR199 rep3
miR RFP P3 rep1
miR RFP P3 rep2
miR RFP P3 rep3
miRandAntimiR rep1
miRandAntimiR rep2
miRandAntimiR rep3
Annotation
CASP14
COL4A1
CSTB
C11orf9
CALD1
APOL1
C3
KRT17
ITGA3
IFI27
RSAD2
CMPK2
ISG15
MX2
SAMD9L
ACVR2B
ITGA1
TGFBR1
NEDD9
BCAM
DDR1
BGN
PADI4
TMPRSS2
COL4A5
LCN2
MICAL3
MUC4
MMP7
PIGR
ZBTB16
RND1
LIN7C
CDH1
PALS1
GAP12
GPRC5A
DCN
TGFBR3
SNAIL
WNT2
IGF1
ITGB4
VIM
PVRL1
WNT7A
CAD11
CTGF
EGR
END1
FN1
KLF2
ITGA2
COL1A1
SMTN
ITGB1
LPAR1
JAG
WNT4
WNT5A
TGFBR2
IL8
LPAR3
IL6
SMO
SM22
antimiR
miR
miR+ antimiR
B
fold difference rel. to scrambled miR
scrambled-miR
miR-199a-5p
antimiR-199a-5p
miR+antimiR
LIN7C
GAP12
PALS1
WNT2
DDR1
ITGA2
CTGF
SNAI1
VIM

ferentiation and proliferation regulators (including MX2, DDR1, ZBP1, DCN, BGN, SM22, JAG1, FN1,VIM, COL4A1, and SNAIL), for a follow-up QPCR. Fig. 1*C* shows a heat map of the QPCR data for 66 genes analyzed. Not all the gene expression changes that were significant in the miR-199a-5p-overexpressing differentiating TEU-2 cells persisted in the miR-overexpressing monolayer TEU-2 cells. However, most miR-199a-5p target genes, including *LIN7C*, *ARHGAP12*, *PALS1*, *DDR1*, and the regulatory *JAG1*, connective tissue growth factor (*CTGF*), and *SNAIL* were similarly regulated regardless of differentiation (Fig. 1*D*), and the overall regulatory pattern indicated that miR-199a-5p had a profound effect on the transcriptome of the transfected TEU-2 cells regardless of differentiation status.

Culturing of the Bladder SMCs Affects Contractile and Regulatory Proteins and Down-regulates Endogenous MiR-199a-5p—Previously, using laser microdissection, we showed that miR-199a-5p was detected in the mature bladder urothelium, and its expression could be up-regulated following activation of cAMP signaling pathways (17). However, its levels in the urothelium are much lower than in the bladder smooth muscle (17), implying an important regulatory role for miR-199a-5p in SMCs.

Cultured bladder SMCs undergo a rapid dedifferentiation accompanied by the loss of contractility and cytoskeletal remodeling (25). We raised primary cultures of the bladder SMCs and assayed them by QPCR for mRNA levels of contractile and regulatory proteins as well as miR-199a-5p (Fig. 2). Already passages 1 and 3 of bladder SMCs displayed a significant down-regulation of caldesmon, SM22, smoothelin, SM α-actin, SM myosin, calponin, and P2X1 receptor mRNAs (Fig. 2*A*). Consequently, the ratio of MYH11 SM2/SM1 isoforms, which is indicative of the differentiated state of the bladder smooth muscle (26), was progressively reduced along with the overall SM myosin heavy chain content (Fig. 2*B*). As the cells regained proliferative activity, the mRNA levels of cyclin D1 and SNAIL were increased along with the ECM components vimentin, fibronectin, and biglycan (Fig. 2, *C* and *D*). We also detected an up-regulation of the validated miR-199a-5p targets LIN7C, ARHGAP12 (17), and WNT2 (27) (Fig. 2*E*). Importantly, culturing of the bladder SMCs caused a significant down-regulation of miR-199a-5p expression levels (Fig. 2*F*). Although these data do not establish a causative link among SM dedifferentiation, down-regulation of miR-199a-5p expression levels, and up-regulation of WNT2 and its effectors, they prompted us to address the potential involvement of the WNT2 regulator miR-199a-5p in SMC differentiation and function.

Inhibition of Endogenous MiR-199a-5p Significantly Decreases Cell Size and Increases SMC Proliferation—To investigate the role of miR-199a-5p in smooth muscle gene expression and function, we altered its levels in primary SMCs using lentiviruses, overexpressing miR-199a-5p or the inhibitory antimiR-199a-5p constructs. To assess the effectiveness of miR-199a-5p induction or inhibition, we first tested the lentivirus constructs in the luciferase assay in HEK293 cells transfected with pmiR-GLO-miR-199a target vector (17). Cells transduced with lentiviruses expressing scrambled miR or antimiR-199a-5p did not show an inhibition of the luciferase activity, whereas the lentivirus overexpressing miR-199a-5p as expected significantly reduced luciferase activity, confirming the synthesis of the mature miRNA (Fig. 3*A*). Co-transduction of HEK293 with miR-199a-5p and scrambled miR-expressing lentiviruses did not significantly alter the luciferase inhibition, whereas in the cells co-expressing miR-199a-5p and antimiR-199a-5p, the luciferase activity was significantly higher than in miR-199a-5p alone, confirming the effective attenuation of this miRNA by its antimiR (Fig. 3*A*).

We transduced low passage bladder SMCs with the scrambled miR control (tagged with RFP), antimiR-199a-5p (tagged with GFP), or both miR-199a-5p and antimiR-199a-5p and studied the cell morphology by live cell imaging (Fig. 3*B*). SMCs expressing antimiR-199a-5p were significantly smaller than controls, and co-expression of antimiR with miR-199a-5p effectively rescued this phenotype (Fig. 3*B*, graph). In addition to the reduced cell size, antimiR-199a-5p-expressing SMCs had a significantly increased proliferation rate compared with the scrambled control and miR-199a-5p as evident by cell count increase and elevated incorporation of BrdU in the antimiR cells (Fig. 3*C*). These results indicate that the inhibition of the endogenous miR-199a-5p in the smooth muscle has profound morphological and proliferative effects.

To evaluate the changes in gene expression resulting from the inhibition of miR-199a-5p, we analyzed a panel of predicted and validated miRNA targets and contractile and regulatory proteins by QPCR (Fig. 4*A*). The heat map summarizes the results of these experiments. The samples of each group (antimiR, miR-199a-5p, and miR + antimiR) clustered together, indicating similarities in gene expression regulation. Validated and high score miR-199a-5p target genes *LIN7C*, *ARHGAP12*, *PALS1*, *WNT2*, and *DDR1* were down-regulated in miR-199a-5p-overexpressing SMCs, up-regulated in antimiR-199a-5p-expressing cells, and normalized in miR + antimiR samples compared with the scrambled miR control (Fig. 4*B*). Interestingly, mRNAs encoding CTGF, transcription factor SNAIL, and ECM protein vimentin as well as integrin A2 were significantly up-regulated in the SMCs transduced with antimiR-199a-5p lentivirus (Fig. 4*B*).

WNT2 Is Regulated by MiR-199a-5p in Bladder SMCs—Many of the proteins up-regulated following miR-199a-5p attenuation, including vimentin, CTGF, and SNAIL, are known components of the WNT signaling pathway. WNT2 is down-

FIGURE 4. **MiR-199a-5p and antimiR-199a-5p have opposite effects on gene expression in bladder SMCs.** *A*, heat map comparing expression of 66 genes in three groups of bladder SMCs: SMCs passage 3 transduced with miR-199a-5p lentivirus (*miR RFP P3*), antimir-199a-5p virus (*AntimiR 199*), and miR-199a-5p and antimiR-199a-5p double transduced virus (*miRandAntimiR*) ($n = 3$ samples per group). The expression levels of genes are shown as -fold changes relative (*rel.*) to control (scrambled miRNA). The square root of the Euclidian distance after centering and rescaling the data (1 − Pearson's correlation) was used to calculate the distance for clustering of the genes and samples. The *rows* correspond to genes, and the *columns* represent the experimental samples. *B*, the graph shows gene expression changes of the validated and high score miR-199a-5p targets and regulated ECM proteins and factors as the averages of triplicates of three independent transduction experiments related to the expression levels of the same genes in the scrambled miR-transduced control samples. *Error bars* represent S.E. (*, $p < 0.05$).

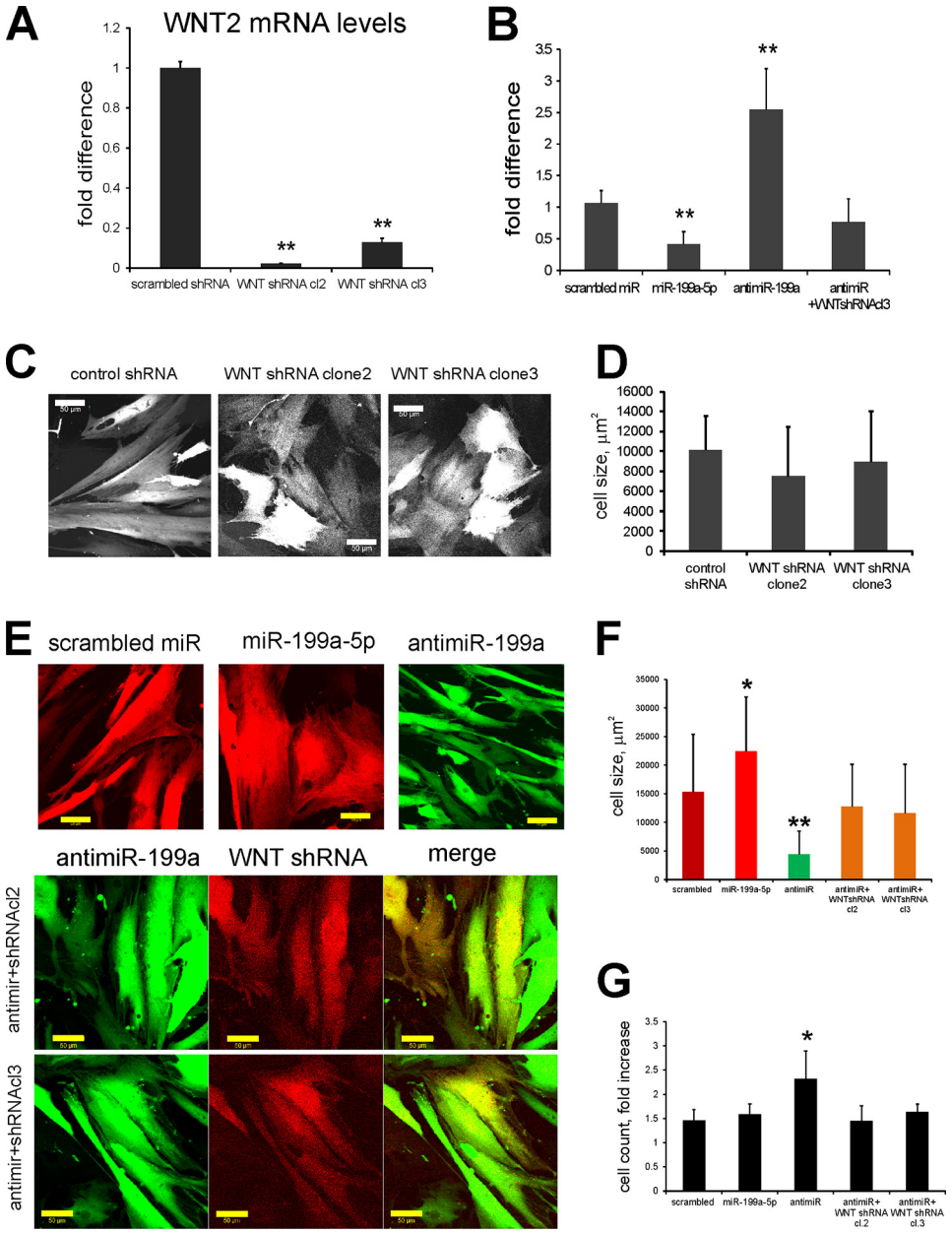

FIGURE 5. **WNT2-specific shRNAs reduce antimiR-199a-5p-mediated up-regulation of WNT2 and normalize cell size and proliferation rates.** *A*, WNT2 is down-regulated by WNT2 shRNA clones 2 and 3. Bladder SMCs primary cultures (passage 1) were stably transduced with lentiviruses expressing different shRNAs specific for the WNT2 sequence. The levels of WNT2 mRNA were analyzed by QPCR in triplicates and compared with the scrambled non-interfering shRNA control. *Error bars* represent S.E. (**, $p < 0.005$). *B*, WNT2-specific shRNAs reduce the antimiR-199a-5p-mediated up-regulation of WNT2. Bladder SMCs were transduced with lentiviruses expressing scrambled miR, miR-199a-5p, or antimiR-199a-5p or co-transduced with antimiR and WNT2 shRNA clone 3. The levels of WNT2 mRNA were analyzed by QPCR and compared with the scrambled miRNA control. Shown are the averages of three separate transduction experiments each performed in triplicate. *Error bars* represent S.E. (**, $p < 0.005$). *C*, SMCs transduced with scrambled shRNA or WNT2 shRNA clones 2 and 3 were examined using an LSM. *Scale bars*, 50 μm. *D*, cell surface area was measured ($n = 100$ cells). Graphs show the averages ± S.D. (*error bars*) (*, $p < 0.05$; **, $p < 0.005$). *E*, bladder SMCs individually expressing scrambled miR (RFP tag), miR-199a-5p (RFP tag), or antimiR-199a-5p (GFP tag) and bladder SMCs co-expressing antimiR-199a-5p (GFP tag) and WNT2 shRNA clone 2 or 3 (mCherry tag) were observed using an LSM at the same magnification. *Scale bars*, 50 μm. *F*, $n = 100$ cells were measured in individually transduced or co-transduced SMCs. The graph shows the average cell surface area in each sample ±S.D. (*error bars*) (*, $p < 0.05$;**, $p < 0.005$). *G*, the bladder SMCs expressing scrambled miR, miR-199a-5p, or antimiR-199a-5p or co-expressing antimiR + WNT2 shRNA clone 2 (*cl2*) or 3 (*cl3*) were seeded in triplicates at 6×10^4 cells/well, and cell count was analyzed 5 days postplating. Data are shown as -fold increase relative to the initial plating density ±S.D. (*error bars*) (*, $p < 0.05$).

regulated by miR-199a-5p and up-regulated by antimiR-199a-5p, consistent with the previous studies validating it as a miR-199a-5p target (27). The pathway analysis of miR-199a-5p-overexpressing TEU-2 cells revealed regulation of the WNT pathway (Table 1), prompting us to investigate the contribution of WNT2 signaling to the morphological and proliferative effects of miR-199a-5p and its antimiR inhibitor.

We tested a panel of WNT2-specific shRNAs and selected two clones effectively down-regulating the endogenous WNT2 mRNA levels in SMCs (Fig. 5*A*). Although the overexpression of miR-199a-5p reduced and that of antimiR-199a-5p increased WNT2 mRNA levels (Figs. 4*B* and 5*B*), the co-expression of antimiR-199a-5p and WNT2 shRNA in the co-transduced primary SMCs reversed the antimiR-mediated increase of WNT2

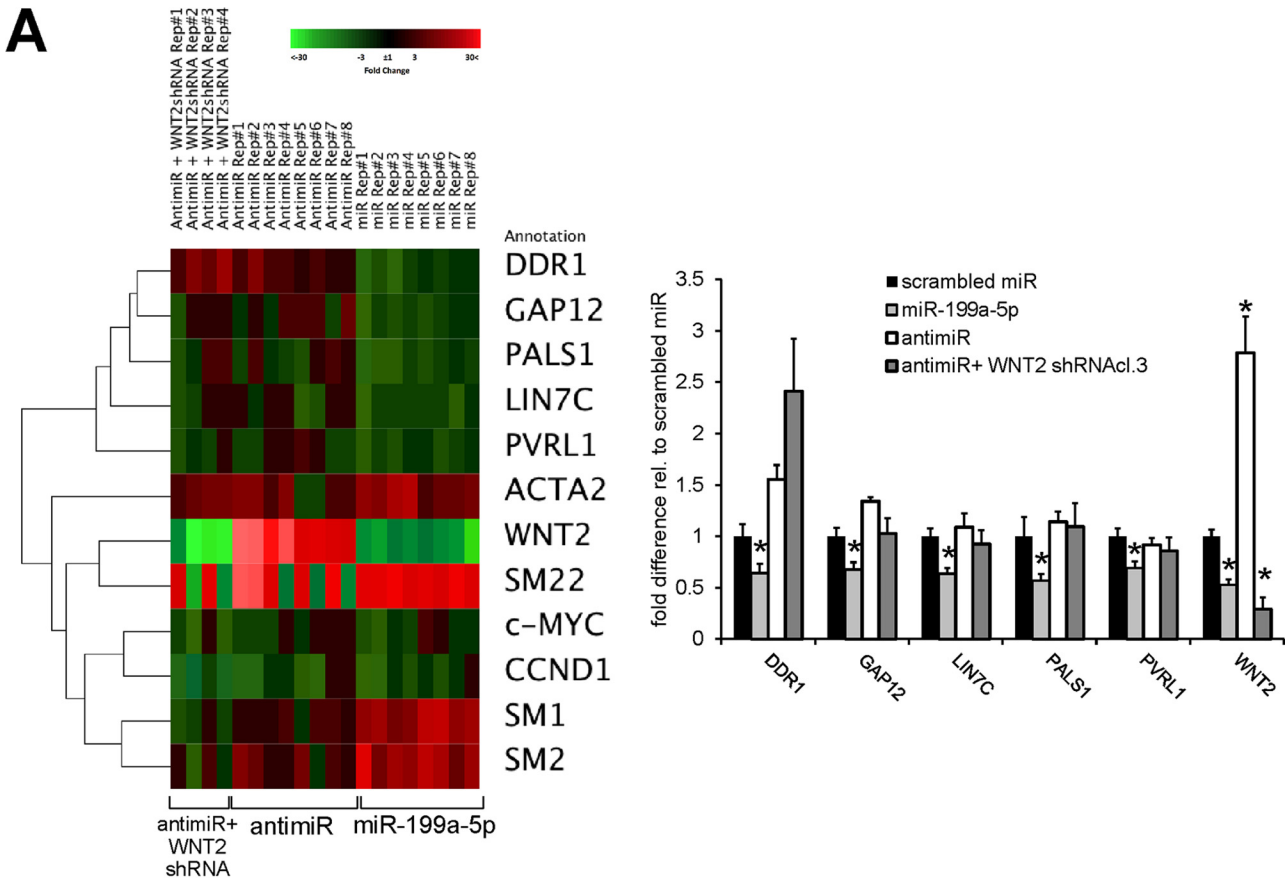
A
AntimiR + WNT2shRNA Rep#1
AntimiR + WNT2shRNA Rep#2
AntimiR + WNT2shRNA Rep#3
AntimiR + WNT2shRNA Rep#4
AntimiR Rep#1
AntimiR Rep#2
AntimiR Rep#3
AntimiR Rep#4
AntimiR Rep#5
AntimiR Rep#6
AntimiR Rep#7
AntimiR Rep#8
miR Rep#1
miR Rep#2
miR Rep#3
miR Rep#4
miR Rep#5
miR Rep#6
miR Rep#7
miR Rep#8
<-30
-3
±1
3
30<
Fold Change
Annotation
DDR1
GAP12
PALS1
LIN7C
PVRL1
ACTA2
WNT2
SM22
c-MYC
CCND1
SM1
SM2
antimiR+ WNT2 shRNA
antimiR
miR-199a-5p
scrambled miR
miR-199a-5p
antimiR
antimiR+ WNT2 shRNAcl.3
fold difference rel. to scrambled miR
3.5
3
2.5
2
1.5
1
0.5
0
DDR1
GAP12
LIN7C
PALS1
PVRL1
WNT2

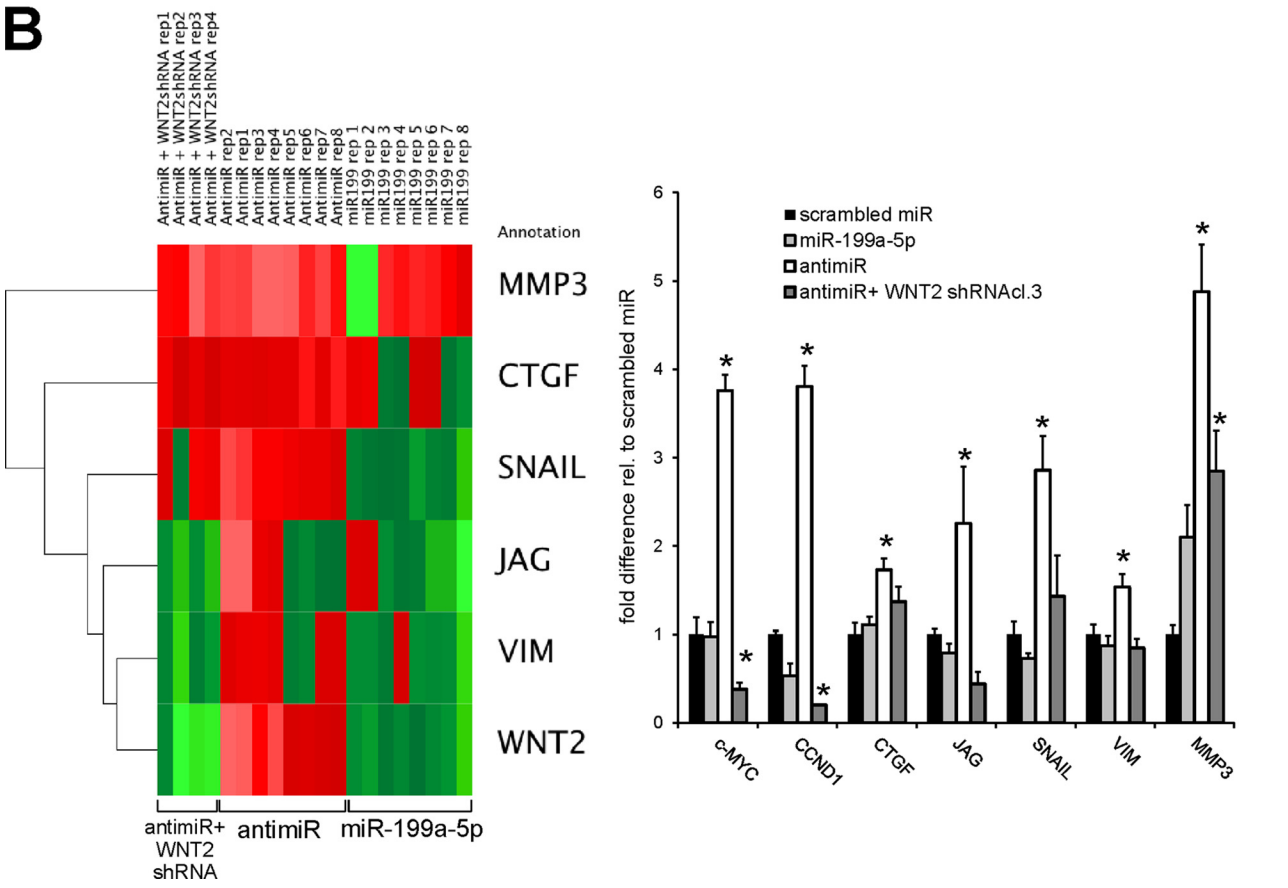
B
AntimiR + WNT2shRNA rep1
AntimiR + WNT2shRNA rep2
AntimiR + WNT2shRNA rep3
AntimiR + WNT2shRNA rep4
AntimiR rep2
AntimiR rep1
AntimiR rep3
AntimiR rep4
AntimiR rep5
AntimiR rep6
AntimiR rep7
AntimiR rep8
miR199 rep 1
miR199 rep 2
miR199 rep 3
miR199 rep 4
miR199 rep 5
miR199 rep 6
miR199 rep 7
miR199 rep 8
Annotation
MMP3
CTGF
SNAIL
JAG
VIM
WNT2
antimiR+ WNT2 shRNA
antimiR
miR-199a-5p
scrambled miR
miR-199a-5p
antimiR
antimiR+ WNT2 shRNAcl.3
fold difference rel. to scrambled miR
6
5
4
3
2
1
0
c-MYC
CCND1
CTGF
JAG
SNAIL
VIM
MMP3

levels (Fig. 5*B*). We studied the effects of WNT2 down-regulation on the bladder SM cell morphology (Fig. 5*C*) and show that WNT2 inhibition did not change the overall cell size (Fig. 5*D*).

To investigate whether the morphological effects of antimiR-199a-5p were due solely to the up-regulation of WNT2 expression, we transduced bladder SMCs with miR-199a-5p- or antimiR-199a-5p-overexpressing lentiviruses as well as co-transduced antimiR-199a-5p with WNT2 shRNA-expressing constructs (clones 2 and 3 were used in separate experiments). Compared with the scrambled miR, overexpression of miR-199a-5p caused a significant increase in the SM cell size (Fig. 5, *E* and *F*); overexpression of antimiR-199a-5p reduced the cell size (Fig. 5, *E* and *F*), whereas antimiR together with WNT2 shRNA clones 2 and 3 restored cell size to the control values (Fig. 5, *E* and *F*). Similarly, the normalization of WNT2 expression levels following co-expression of antimiR-199a with WNT2 shRNA reduced the proliferation rates back to the control levels (Fig. 5*G*).

Manipulation of WNT2 Levels in the AntimiR-199a-5p-expressing Cells Affects the Expression of WNT2 Signaling Pathway Components—To examine whether the rescue of the morphology and proliferation rates by WNT2 shRNAs in antimiR-199a-5p-experessing SMCs was due to the attenuation of the WNT signaling pathway, we investigated the mRNA levels of the miR-199a-5p target proteins and genes regulated by WNT2 as well as contractile proteins. With the exception of WNT2 itself, all other validated miR-199a-5p targets remained unaffected by the shRNA-mediated decrease of WNT2 mRNA levels (Fig. 6*A*). Conversely, contractile proteins and SM markers SM α-actin, SM myosin heavy chain (isoforms SM1 and SM2), and SM22 protein observed to be up-regulated in miR-199a-5p-expressing cells were not strongly altered in antimiR-199a-5p-expressing cells compared with scrambled miR control (Fig. 6*A*). Importantly, the up-regulated mRNA levels of WNT-dependent proteins SNAIL1, JAG1, CTGF, cyclin D1, and vimentin were significantly attenuated after the addition of WNT2 shRNA (Fig. 6*B*). These results show that the components of the WNT signaling pathway and genes up-regulated as the result of its activation are controlled by miR-199a-5p via its ability to influence WNT2 levels.

Overexpression of MiR-199a-5p in Bladder SMCs Increases the Expression of Contractile and Cytoskeletal Elements via Inhibition of WNT2—Cytoskeleton remodeling pathways were high on the list of the top miR-199a-5p-dependent pathways in TEU-2 cells (Table 1), and an up-regulation of SM markers smoothelin and SM22 was detected in miR-overexpressing differentiated TEU-2 cells by mRNA-seq (Fig. 1*B*) and QPCR (Fig. 1*C*). Previously, we have observed a significant increase in stress fiber formation in miR-199a-5p-overexpressing TEU-2 cells (17), indicating cytoskeletal rearrangements.

We modulated the levels of the endogenous miR-199a-5p using recombinant lentiviruses and examined the filamentous actin in the bladder SMCs. The cells overexpressing miR-199a-5p showed prominent actin stress fibers (Fig. 7*A*). Interestingly, the down-regulation of WNT2 with specific shRNAs also caused strong stress fiber formation accompanied by cell spreading (Fig. 7*A*). In contrast, the cells overexpressing antimiR-199a-5p, although smaller in size, displayed a less pronounced phalloidin staining, and the actin fiber formation was restored along with the cell size increase in antimiR + WNT2 shRNA-co-transduced SMCs (Fig. 7*B*). The mRNA levels of SM α-actin, SM myosin heavy chain isoforms, and SM22 were significantly up-regulated in the miR-199a-5p-overexpressing cells (Fig. 7*C*). The protein levels of SM myosin heavy chain and SM α-actin were also considerably elevated, whereas the smooth muscle-nonspecific l-caldesmon remained unchanged in the examined samples (Fig. 7*D*). The levels of h-caldesmon are rapidly decreased in cultured SMCs compared with the functional smooth muscle (28). We observed an up-regulation of h-caldesmon in miR-199a-5p-overexpressing SMC and its significant down-regulation in antimiR-expressing cells (Fig. 7*E*), indicating an antimiR-induced acceleration of SMC dedifferentiation.

MiR-199a-5p Promotes the Expression of MRTF-A-dependent Smooth Muscle Regulatory Id3 Protein—Activation of cytoskeleton remodeling pathways in miR-199a-5p-overexpressing SMCs impelled us to investigate the involvement of the actin dynamics-responsive MRTF-A in the gene expression regulation of smooth muscle-specific contractile proteins. We observed an increase in the levels of Rac1 activation (Fig. 8*A*) and some nuclear localization of MRTF-A in miR-199a-5p SMCs (Fig. 8*B*, *arrows*). MRTF-A exerts it functions following nuclear relocalization rather than an expression level increase (29); consequently, we did not detect significant changes of MRTF-A mRNA levels in miR-199a-5p-expressing cells (Fig. 8*C*). However, there was a significant up-regulation of transcription of MRTF-A-dependent myosin regulatory light chain 9 (MYL9) (30) and Id3 (31) (Fig. 8*C*).

Id3 is an important regulator of smooth muscle differentiation program (32). It is localized in the nucleus of bladder SMCs (Fig. 8*D*), and Id3 protein levels are increased in miR-199a-5p-overexpressing cells (Fig. 8*E*), consistent with an increase of SM differentiation markers MYH11, ACTA2, and SM22.

Increased Expression of Myocardin and Myocardin-stimulated Genes in MiR-199a-5p-overexpressing SMCs—SM α-actin, SM myosin heavy chain, SM22, and h-caldesmon are induced by serum response factor (SRF) in complex with its transcriptional co-activator myocardin; therefore, to understand the mechanisms of miR-199a-5p-induced up-regulation of their gene expression (Fig. 7), we studied the expression of

FIGURE 6. **Co-expression of antimiR-199a-5p and WNT2 shRNA affects the WNT2-regulated genes but not the other miR-199a-5p targets.** Shown are heat map and cluster analysis of bladder SMCs (passage 3) transduced with scrambled miR virus (control), miR-199a-5p virus (eight replicates *(Rep)*; *miR*), antimir-199a-5p virus (eight replicates; *AntimiR*), and antimir-199a-5p co-transduced with WNT2 shRNA (four replicates; *antimiR + WNT shRNA*). -Fold change values relative (*rel.*) to the scrambled miR control were used for heat map generation. The graphs show the average -fold change values of two independent transduction experiments performed in triplicates for miR-199a-5p and antimiR samples and two transduction experiments performed in duplicates for antimiR + WNT2 shRNA clone 3 (*cl.3*) ±S.E. (*error bars*) (*, $p < 0.05$). *A*, results for miR-199a-5p targets and contractile and cell cycle proteins; *B*, results for WNT2 and the genes it regulates.

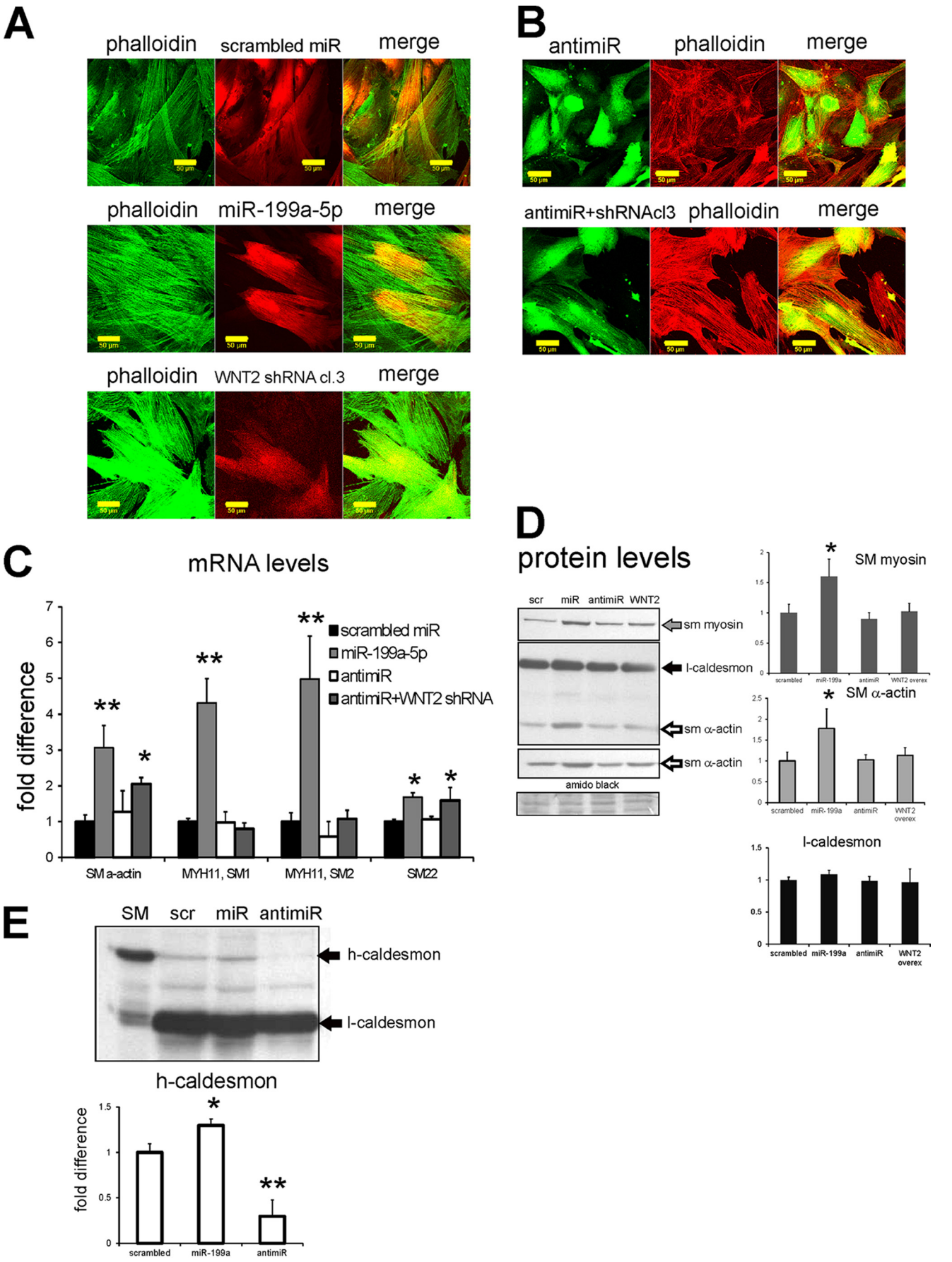
A
phalloidin
scrambled miR
merge
phalloidin
miR-199a-5p
merge
phalloidin
WNT2 shRNA cl.3
merge
B
antimiR
phalloidin
merge
antimiR+shRNAcl3
phalloidin
merge
C
mRNA levels
fold difference
scrambled miR
miR-199a-5p
antimiR
antimiR+WNT2 shRNA
SM a-actin
MYH11, SM1
MYH11, SM2
SM22
D
protein levels
scr
miR
antimiR
WNT2
sm myosin
l-caldesmon
sm α-actin
sm α-actin
amido black
SM myosin
SM α-actin
l-caldesmon
scrambled
miR-199a
antimiR
WNT2 overex
E
SM
scr
miR
antimiR
h-caldesmon
l-caldesmon
h-caldesmon
fold difference
scrambled
miR-199a
antimiR

myocardin in these cells. The mRNA levels of myocardin and its regulated genes SM γ-actin (*ACTG2*), desmin (*DES*), transforming growth factor-β1-induced transcript 1 (*TGFB1I1*), and cell cycle inhibitory protein p21 (*CDKN1A*) were significantly up-regulated in miR-199a-5p-overexpressing SMCs (Fig. 9*A*). Myocardin was also increased at the protein level (Fig. 9*B*), and its nuclear localization was confirmed by immunofluorescence (Fig. 9*C*).

Although antimiR-expressing cells show myocardin mRNA levels similar to control levels, we observed a down-regulation of myocardin targets desmin, TGFB1I1, and h-caldesmon indicative of the inhibition of myocardin-mediated gene expression. We analyzed the mRNA levels of myocardin inhibitors ELK1, FOXO4, and Krüppel-like factor 4 (KLF4) and show a significant up-regulation of KLF4 mRNA levels in the antimiR-199a-5p-expressing SMCs (Fig. 9*D*) and a concomitant reduction of its transcription in miR-199a-5p-overexpressing cells. KLF4 is a WNT-dependent gene (33), and its expression pattern was consistent with that of Axin2, another WNT target (Figs. 9*D* and 8*C*).

Modulation of WNT2 Signaling in Bladder SMCs Mimics the Morphologic and Proliferative Effects of MiR-199a-5p Expression Changes—Having established that the up-regulation of WNT2 was the crucial factor responsible for the morphological and proliferative effects of miR-199a-5p inhibitor, we sought to model these changes by ectopically overexpressing WNT2 protein. The cDNA sequence of human WNT2 was PCR-amplified and expressed as a fusion with copepod *Pontellina plumata* copGFP, which acted as a direct reporter of the protein expression. Transduced bladder SMCs showed a significant increase of WNT2 expression at the mRNA and protein levels (Fig. 10*A*). Analysis of cell size and morphology revealed similarities between antimiR-199a-5p- and WNT2-overexpressing cells (Fig. 10*B*); both caused a significant reduction of cell size compared with the scrambled miR control (Fig. 10*C*).

The effect of activation and inhibition of WNT signaling pathway was further tested in control and transduced SMCs exposed to recombinant human WNT 2 protein (100 ng/ml) or DKK1 protein (50 ng/ml) for 48–72 h. Incubation of scrambled miR-, miR-199a-5p-, and antimiR-199a-5p-expressing SMCs with recombinant WNT2 caused a significant decrease of cell size (Fig. 10, *D* and *E*) and an increase in proliferation rates (Fig. 10*F*). Addition of WNT inhibitor DKK1 did not significantly alter the size of the control- or miR-199a-5p-expressing cells with low endogenous WNT levels (Fig. 10*E*); however, DKK1 had a pronounced effect on the antimiR-expressing cells where it antagonized the activated WNT signaling and as a consequence significantly increased the cell size, bringing it close to the control level (Fig. 10, *D* and *E*).

Activation and inhibition of WNT signaling in WNT2- and DKK1-treated SMCs was confirmed by QPCR of WNT-regulated genes *Axin2* and *KLF4* (Fig. 10*G*). *Axin2* was significantly up-regulated in the WNT2-treated SMCs and down-regulated in the DKK1-treated SMCs, and *KLF4* showed a tendency to be up-regulated in the WNT2-treated SMCs and a significant down-regulation in the DKK1-treated cells.

DISCUSSION

MicroRNA miR-199a-5p is expressed in a broad array of tissues, including the brain, liver, vascular and visceral smooth muscle, ovarian and testicular tissue, cardiomyocytes, and endothelial cells (34). In cardiomyocytes, it down-regulates hypoxia-inducible factor 1α and sirtuin 1 (35) and is one of the factors regulating cell size: its overexpression in cardiomyocytes leads to hypertrophy (36). It is transcribed as antisense to dynamin 3 within introns on chromosome 1 (1q24.3) and dynamin 2 on chromosome 19 (27, 37). Expression of miR-199a-5p is regulated by a variety of stimuli: hypoxia and AKT signaling cause its rapid decrease and an up-regulation of its targets (35). Activation of the cAMP-PKA pathway for example following stimulation of β_2-adrenergic receptors induces miR-199a-5p synthesis in cardiomyocytes and bladder urothelium (17). TGFβ, which is increased in the majority of diseases accompanied by fibrosis (38, 39), is another strong inducer of miR-199a-5p synthesis. MiR-199a-5p attenuated expression of CAV1, a critical mediator of pulmonary fibrosis (40), implicating it in the pathogenesis of fibrosis in lung and hepatic tissue.

Previously, we have shown that upon overexpression in urothelial and bronchial epithelial cells miR-199a-5p impaired correct tight junction formation and led to an increased epithelial permeability due to a significant down-regulation of LIN7C, ARHGAP12, PALS1, RND1, and PVRL1, the key proteins involved in tight junction, adherens junction, and actin dynamics (17). The expression of miR-199a-5p in differentiating TEU-2 cells led to cell flattening and delayed formation of a multilayered epithelium and induced stress fibers. Notably, the effects of miR-199a-5p during adherens junction/tight junction formation were pleiotropic as the rescue experiments with some of its target proteins ameliorated but did not abolish the miR-199a-5p-induced decrease of urothelial integrity.

Here we carried out a comprehensive mRNA-seq analysis of the TEU-2 urothelial cell line overexpressing miR-199a-5p and demonstrated 1646 genes differentially expressed following miRNA transfection (p value <0.05,

FIGURE 7. **MiR-199a-5p influences actin dynamics and increases levels of SM-specific contractile proteins.** Fibrillar actin was stained in fixed, permeabilized SMCs using Alexa Fluor 488-conjugated (*A*) or Cy3-conjugated (*B*) phalloidin. Images were taken at the same magnification, exposure, and amplifier gain settings. *Scale bars*, 50 μm. *C*, mRNA levels of SM α-actin, myosin heavy chain SM isoforms SM1 and SM2, and SM22 protein were analyzed by QPCR in the samples of bladder SMCs expressing miR-199a-5p or antimiR-199a-5p or co-expressing antimiR with WNT2 shRNA clone 3 and compared with the scrambled miR control. Shown are data of two independent lentivirus transductions in triplicates ±S.E. (*error bars*) (*, $p < 0.05$; **, $p < 0.005$). *D*, the miR-199a-5p-, antimiR-199a-5p-, WNT2-, and control scrambled (*scr*) miR-expressing cell lysates were analyzed by SDS-PAGE under equal loading (20 μg of total protein/lane) followed by Western blotting with anti-SM myosin, anti-SM α-actin, and anti-caldesmon antibodies as specified. The protein levels were quantified as described under "Experimental Procedures." The intensity of each band of interest was normalized to Amido Black staining (shown) and related to the scrambled miR. The graphs show an average of three experiments ±S.E. (*error bars*). Statistically significant differences from the scrambled miR control are indicated (*, $p < 0.05$). *E*, the bladder SM sample and the scrambled miR-, miR-199a-5p-, and antimiR-199a-5p-expressing SMC lysates were analyzed by Western blotting with anti-caldesmon antibody. The bands of h- and l-caldesmon are indicated. The intensity of the h-caldesmon band in SMC samples was normalized to l-caldesmon and related to the normalized scrambled miR values. The graph shows an average of six experiments ±S.E. (*error bars*). Statistically significant differences from the scrambled miR control are indicated (*, $p < 0.05$; **, $p < 0.005$). *overex*, overexpressing.

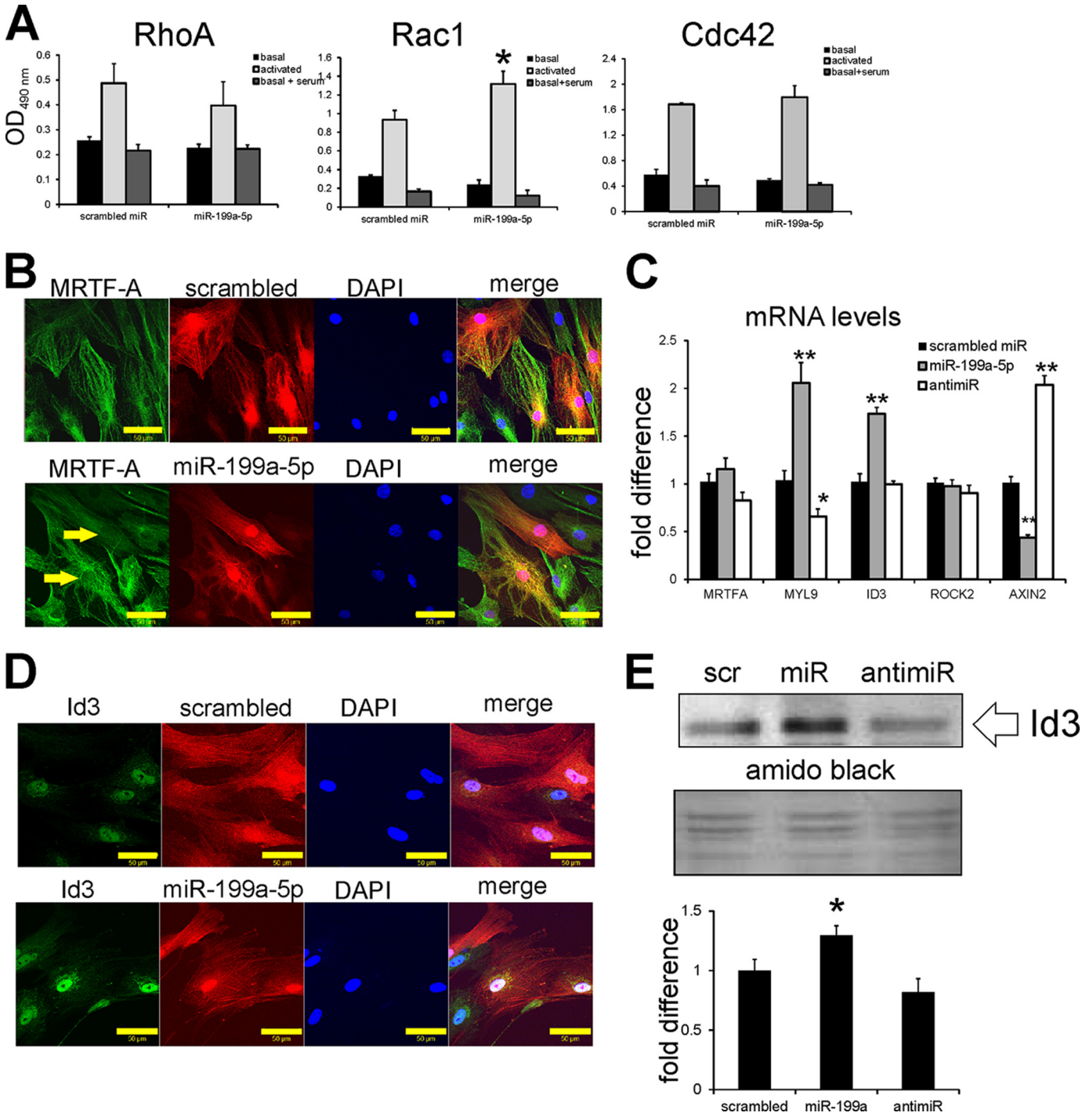

FIGURE 8. **Activation of MRTF-A-dependent gene expression in miR-199a-5p-overexpressing SMCs.** *A*, levels of basal and activated Rho GTPases RhoA, Rac1, and Cdc42 were measured in scrambled miR- and miR-199a-5p-transduced SMCs using G-LISA as recommended by the manufacturer. Shown are averages of three experiments. *Error bars* represent S.E. (*, $p < 0.05$). *B*, localization of MRTF-A in transduced SMCs (*red*) was examined by immunofluorescence with anti-MRTF-A monoclonal antibodies (*green*). Nuclei were stained with 4′,6-diamidino-2-phenylindole (*DAPI*). *Arrows* indicate MRTF-A-positive nuclei of miR-199a-5p-expressing cells. *Scale bars*, 50 μm. *C*, mRNA levels of MRTF-A, its targets MYL9 and Id3, ROCK2, and WNT-dependent Axin2 were determined by QPCR and expressed as -fold ratio to scrambled miR. Shown are averages of four independent transduction experiments each in triplicates. *Error bars* represent S.E. (*, $p < 0.05$; **, $p < 0.005$). *D*, immunofluorescence staining of scrambled miR- and miR-199a-5p-transduced SMCs (*red*) with anti-Id3 antibodies (*green*). Images were taken at the same settings (amplitude and detector gain). *Scale bars*, 50 μm. *E*, scrambled (*scr*) miR-, miR-199a-5p-, and antimiR-199a-5p-expressing SMC lysates were analyzed by Western blotting with anti-Id3 antibody. The Id3 band was normalized to Amido Black staining of the same samples and related to the normalized scrambled miR values. The graph shows an average of three experiments ±S.E. (*error bars*). Statistically significant differences from the scrambled miR control are indicated (*, $p < 0.05$).

false discovery rate <0.05). The pathway analysis performed using the full transcriptome data as well as bioinformatics predictions of the validated and high score miR-199a-5p targets genes, including those expressed in TEU-2 cells, identified TGF, WNT, and cytoskeletal remodeling as the major miR-199a-5p-regulated pathway.

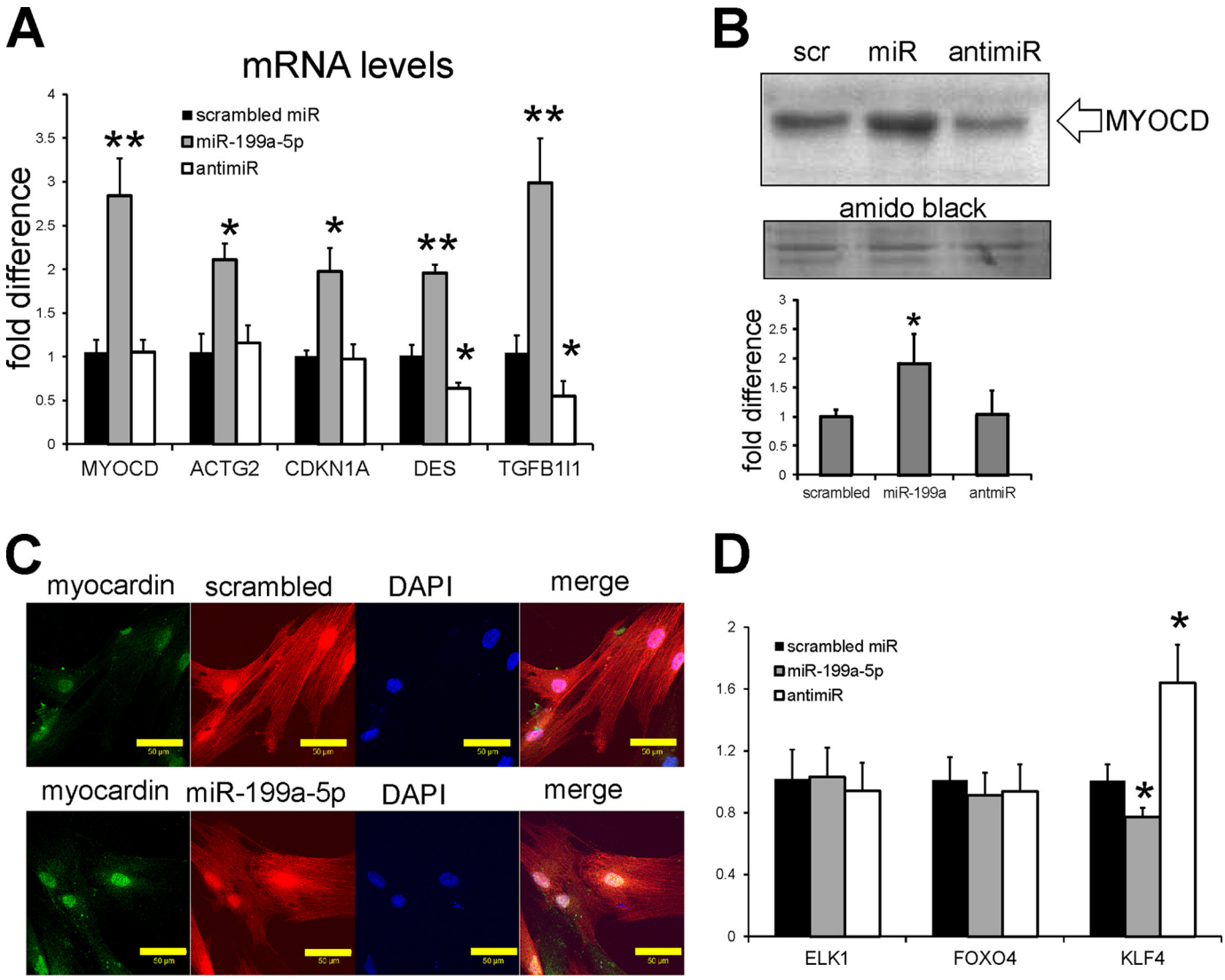

FIGURE 9. **Up-regulation of myocardin and activation of myocardin-dependent genes are accompanied by changes in KLF4 expression.** *A*, mRNA levels of myocardin (*MYOCD*) and the genes it stimulates, SM γ-actin (*ACTG2*), desmin (*DES*), transforming growth factor-β1-induced transcript 1 (*TGFB1I1*), and cell cycle inhibitory protein p21 (*CDKN1A*) were analyzed by QPCR, normalized to 28 S rRNA, and related to the levels in scrambled miR-transduced cells. Shown are the averages of four independent transduction experiments each in triplicates. *Error bars* represent S.E. (*, $p < 0.05$; **, $p < 0.005$). *B*, protein levels of myocardin were determined by Western blotting with anti-myocardin antibody. The myocardin band was normalized to Amido Black staining of the same samples and related to the normalized scrambled miR values. The graph shows an average of three experiments ±S.E. (*error bars*). Statistically significant differences from the scrambled (*scr*) miR control are indicated (*, $p < 0.05$). *C*, immunofluorescence staining of scrambled miR- and miR-199a-5p-transduced SMCs (*red*) with anti-myocardin antibodies (*green*). Images were taken at the same settings (amplitude and detector gain). *Scale bars*, 50 μm. *D*, mRNA levels of myocardin repressors ELK1, FOXO4, and KLF4 were analyzed by QPCR, normalized to 28 S rRNA, and related to the levels in scrambled miR-transduced cells. Shown are averages of four independent transduction experiments each in triplicates. *Error bars* represent S.E. (*, $p < 0.05$).

Previously, we showed that miR-199a-5p was highly expressed in the bladder smooth muscle layer (17), indicative of its importance for the bladder SMC function. Based on the concept that miRNAs regulate signaling networks rather than individual genes (41), we sought to validate our analysis of miR-199a-5p-dependent pathways in a different cell system: human bladder SMCs. Using primary cultures of bladder SMCs, we show that, concomitant with SMC dedifferentiation, miR-199a-5p expression decreased, and the levels of its target mRNAs increased. To identify the signaling pathways affected by this regulatory miRNA, we experimentally manipulated the levels of the endogenous miR-199a-5p in the bladder SMC cultures. Gene expression analysis of the miR-199a-5p- and anti-miR-199a-5p-transduced SMCs confirmed the regulation of genes identified in the differentiated and monolayer TEU-2 cultures ectopically expressing miR-199a-5p. Specifically, DDR1 and WNT2, previously validated as miR-199a-5p targets (27, 42), as well as LIN7C, ARHGAP12, and PALS1 shown in our earlier study were significantly and reversely changed in the bladder SMCs following the alteration of the endogenous miRNA levels by overexpression of miR-199a-5p or antimiR-199a-5p. In line with these data, another study demonstrated that overexpression of miR-199a-5p led to decreased DDR1, MMP2, N-cadherin, and vimentin expression (43). In contrast, we did not observe an inhibitory effect of miR-199a-5p on mRNA and protein levels of caveolin 1 (40) either in TEU-2 cells or in the bladder SMCs, which could be attributed to the tissue specificity of the miRNA effects.

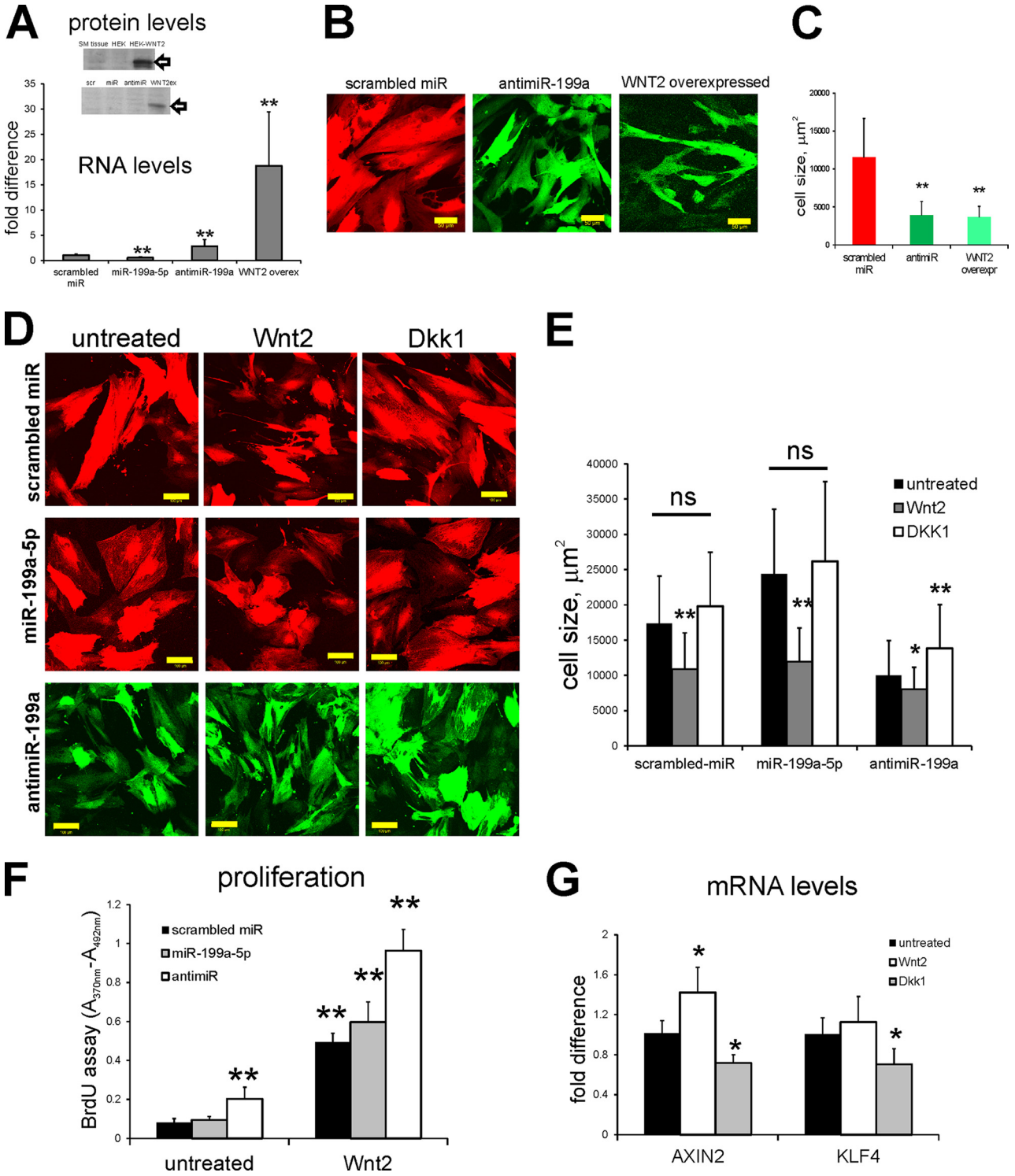

FIGURE 10. **Modulation of WNT2 signaling in bladder SMCs and its effect on cell size, proliferation, and gene expression.** *A*, overexpression (*overex*) of WNT2 in bladder SMCs. QPCR was used to determine the mRNA levels of WNT2 in bladder SMCs expressing scrambled (*scr*) miR control, miR-199a-5p, antimiR-199a-5p, and WNT2 protein. Graphs show the results related to scrambled miR control in three independent experiments ±S.E. (**, $p < 0.005$). Western blotting with anti-WNT2 polyclonal antibodies detects WNT2 protein in HEK293 cells transfected with WNT2-overexpressing plasmid and in bladder SMCs transduced with WNT2-expressing lentivirus. The position of WNT2 protein is indicated with an *arrow*. *B*, WNT2-overexpressing bladder SMCs were imaged live at the same magnification as scrambled miR control- and antimiR-199a-5p-expressing cells. *Scale bars*, 50 μm. *C*, cell size of the WNT2- and antimiR-199a-5p-expressing SMCs compared with the scrambled miR control ±S.D. (*error bars*) (**, $p < 0.005$). *D*, scrambled miR-, miR-199a-5p-, and antimiR-transduced SMCs were treated with human recombinant WNT2 (100 ng/ml) and DKK1 (50 ng/ml) for 72 h before examining live using an LSM. *Scale bars*, 100 μm. *E*, cell surface area was measured ($n = 60$ cells). Graphs show the averages ± S.D. (*error bars*) (*, $p < 0.05$; **, $p < 0.005$; *ns*, not significant). *F*, cell proliferation following WNT2 treatment was analyzed by a BrdU incorporation assay. Cells were seeded at 2×10^3 cells/well ($n = 6$ per measurement), grown for 72 h, and treated with recombinant WNT2 for a further 48 h followed by BrdU labeling and a proliferation assay. The graph shows averages of three measurements. Differences from untreated scrambled miR are indicated (**, $p < 0.005$). *G*, mRNA levels of WNT-dependent *Axin2* and *KLF4* genes were determined by QPCR in untransduced bladder SMCs treated with recombinant WNT2 or DKK1 for 48 h. Average ($n = 3$) -fold differences from the mRNA levels in untreated SMCs ±S.E. (*error bars*) are shown (*, $p < 0.05$).

The pivotal role of WNT2-mediated signaling as the main pathway influenced by miR-199a-5p in the bladder smooth muscle was demonstrated by the gene knockdown and overexpression experiments. Attenuation of the endogenous miR-199a-5p levels with antimiR caused a significant reduction of the bladder SMC cell size and increased cell proliferation. We show that these changes were caused by the loss of miR-specific inhibition and the subsequent increase of WNT2 expression levels, leading to up-regulation of its effectors cyclin D1, c-myc, JAG1, and SNAIL. Although WNT2 is one among the numerous miR-199a-5p-regulated proteins, the importance of its up-regulation and the subsequent activation of the WNT signaling pathway was confirmed by gene knockdown experiments: when WNT2 levels up-regulated in the antimiR-199a-5p-expressing cells were restored by the co-expression of WNT2-specific shRNAs, both the cell size and the proliferation rates returned to control levels. In contrast, overexpression of WNT2 protein or treating the cells with recombinant WNT2 caused effects similar to those of antimiR-199a-5p, leading to a remarkable cell size reduction and accelerated proliferation. Conversely, overexpressing miR-199a-5p in the bladder SMCs caused a significant increase of the cell size, enhanced stress fiber formation, and considerably increased the synthesis of contractile and SM-specific proteins SM α-actin, SM myosin, SM22, and h-caldesmon. The importance of miR-199a-5p in the regulation of the smooth muscle cell size reported here is supported by an observation that its expression correlated with hypertrophy, but not fibrosis, in hypertrophic cardiomyopathy (44).

WNT/Frizzled/β-catenin signaling regulates embryonic development and tissue homeostasis, and its dysregulation is a common cause of cancers (45). WNT2 plays a role in SM and cardiac muscle differentiation: it is strongly up-regulated during cardiomyocyte differentiation and plays a strong positive stage-specific role in cardiogenesis through the non-canonical WNT pathway in murine embryonic stem (ES) cells (46). Mice deficient for WNT2 displayed vascular abnormalities, including defective placental vasculature (47), and it was shown that WNT2 signaling was necessary and sufficient for activation of a transcriptional and signaling network critical for smooth muscle specification and differentiation, including myocardin/MRTF-B and the signaling factor FGF10 (48). WNT2 functions at multiple stages of development during ES cell differentiation and the commitment and diversification of mesoderm (49).

In contrast to embryonic development, in differentiated SMCs, activation of WNT induced cell proliferation, whereas its inhibition improved muscle contractility: a significant induction of WNT2 and WNT4 mRNA was detected in proliferating vascular SMCs (50), and inhibition of WNT signaling improved contractile function in experimental models of myocardial infarction (51). Our data support the latter finding: we show that WNT2 inhibition by miR-199a-5p occurred simultaneously with activation of both myocardin- and MRTF-A-dependent SM differentiation programs in SMCs overexpressing miR-199a-5p. We propose that these effects originate from two separate facets of miR-199a-5p function, namely its ability to regulate the cytoskeleton dynamics, leading to the activation of MRTF-A-induced gene expression, and its function as an inhibitor of WNT signaling, resulting in the attenuation of KLF4 synthesis (Fig. 11). KLF4 is a potent repressor of both myocardin expression and myocardin-induced activation of SM genes (52). It is not a direct target of miR-199a-5p, but as a WNT-responsive gene (33), it is amendable to modulation following miR-199a-5p-mediated WNT2 down-regulation (Fig. 11). Our model does not exclude the involvement of further miR-regulated pathways affecting the SRF/myocardin gene expression program. Specifically, the link between KLF4 and miR-199a-5p awaits further study.

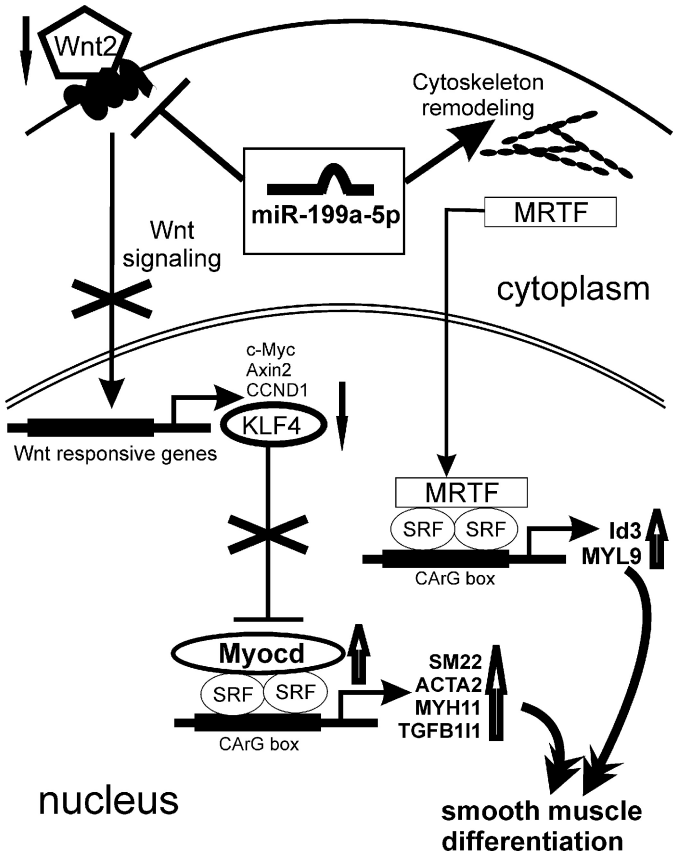

FIGURE 11. **Model of miR-199a-5p in smooth muscle differentiation and hypertrophy.** Increased expression of miR-199a-5p in smooth muscle cells has two main consequences: it affects WNT signaling by down-regulating WNT2 and influences cytoskeleton remodeling. 1) Inhibition of the WNT signaling pathway leads to down-regulation of KLF4, a WNT-dependent repressor of both myocardin synthesis and transcription of SRF/myocardin (*Myocd*)-stimulated genes. The KLF4 decrease leads to elevation of myocardin levels; together with SRF, myocardin then induces genes encoding SM-specific and contractile proteins, including SM22, SM α-actin (*ACTA2*), SM myosin heavy chain (*MYH11*), and transforming growth factor-β1-induced transcript 1 (*TGFB1I1*). 2) MiR-199a-5p-regulated cytoskeleton remodeling activates actin-dependent MRTF-A, which translocates to the nucleus, associates with SRF, and stimulates expression of MYL9 and Id3. Id3 is a part of a regulatory network promoting smooth muscle differentiation. The resulting increase in synthesis of contractile and structural proteins leads to SMC hypertrophy.

Recently, it was shown that miR-199a-5p was regulated in an SRF-dependent manner like the other muscle miRNAs, including miR-1, miR-133a/b, miR-143, miR-145, miR-206, and miR-486 (53). Interestingly, similar to miR-199a-5p, muscle-specific miR-1 suppresses WNT signaling and promotes differentiation of cardiomyocytes by modulating the activities of WNT and FGF signaling pathways (54). Our results suggest the existence of a positive feedback loop between SRF/myocardin and miR-199a-5p that promotes the SM-specific gene expression.

Previously, miR-199a-5p has been described as a negative regulator of keloid fibroblast (55) and endometrial mesenchymal stem cell (56) proliferation. Our study demonstrates that the ability of miR-199a-5p to modulate WNT signaling regulates proliferation of the bladder smooth muscle.

In the striated muscle, overexpression of miR-199a-5p promoted myoblast but not myotube proliferation (27), resulting in abnormal myofiber disruption and inhibition of myogenic differentiation. Here we report an increase of Id3 mRNA and protein levels in miR-199a-5p-overexpressing SMCs. Id3 is an important regulator of gene expression, playing a critical role in SM differentiation (32, 57). Id3 has been shown to inhibit striated muscle differentiation, preventing myoblast-myotube conversion (58) by antagonizing the promyogenic activities of Myf5 and Pax7 (32). Up-regulation of Id3 observed here offers an additional argument supporting the importance of miR-199a-5p in dystrophic muscle.

Our results point to the crucial role of miR-199a-5p in the WNT2-mediated regulation of proliferative and differentiation processes in the bladder smooth muscle. Recent evidence suggests that sustained WNT pathway reactivation is linked to the pathogenesis of fibrotic diseases (59). By regulating WNT-dependent cytoskeleton remodeling pathways, miR-199a-5p may behave as a key modulator of smooth muscle hypertrophy and fibrosis, which are relevant for bladder organ remodeling.

Acknowledgments—We are grateful to Prof. David J. Klumpp (Northwestern University, Chicago, IL) for providing the TEU-2 cell line, Dr. Matthew S. Alexander (Boston Children's Hospital, Boston, MA) for the stimulating discussions and miRNA lentiviral vectors, Carla Ruckstuhl for help with virus preparation, and Irena Klima for technical assistance.

REFERENCES

1. Slobodov, G., Feloney, M., Gran, C., Kyker, K. D., Hurst, R. E., and Culkin, D. J. (2004) Abnormal expression of molecular markers for bladder impermeability and differentiation in the urothelium of patients with interstitial cystitis. *J. Urol.* **171,** 1554–1558
2. Sanchez Freire, V., Burkhard, F. C., Kessler, T. M., Kuhn, A., Draeger, A., and Monastyrskaya, K. (2010) MicroRNAs may mediate the down-regulation of neurokinin-1 receptor in chronic bladder pain syndrome. *Am. J. Pathol.* **176,** 288–303
3. Adam, R. M. (2006) Recent insights into the cell biology of bladder smooth muscle. *Nephron Exp. Nephrol.* **102,** e1–e7
4. Andersson, K. E., and Arner, A. (2004) Urinary bladder contraction and relaxation: physiology and pathophysiology. *Physiol. Rev.* **84,** 935–986
5. Hypolite, J. A., Chang, S., Zheng, Y., DiSanto, M. E., Zderic, S. A., Wein, A. J., and Chacko, S. (2006) Partial bladder outlet obstruction induces urethral smooth muscle hypertrophy and decreased force generation. *J. Urol.* **175,** 777–782
6. Myers, J. B., Dall'era, J. E., Koul, S., Kumar, B., Khandrika, L., Flynn, B. J., and Koul, H. K. (2009) Biochemical alterations in partial bladder outlet obstruction in mice: up-regulation of the mitogen activated protein kinase pathway. *J. Urol.* **181,** 1926–1931
7. Chacko, S., Chang, S., Hypolite, J., Disanto, M., and Wein, A. (2004) Alteration of contractile and regulatory proteins following partial bladder outlet obstruction. *Scand. J. Urol. Nephrol. Suppl.* **215,** 26–36
8. Bartel, D. P. (2009) MicroRNAs: target recognition and regulatory functions. *Cell* **136,** 215–233
9. Lu, M., Zhang, Q., Deng, M., Miao, J., Guo, Y., Gao, W., and Cui, Q. (2008) An analysis of human microRNA and disease associations. *PLoS One* **3,** e3420
10. Wilmott, J. S., Zhang, X. D., Hersey, P., and Scolyer, R. A. (2011) The emerging important role of microRNAs in the pathogenesis, diagnosis and treatment of human cancers. *Pathology* **43,** 657–671
11. Gheinani, A. H., Burkhard, F. C., and Monastyrskaya, K. (2013) Deciphering microRNA code in pain and inflammation: lessons from bladder pain syndrome. *Cell. Mol. Life Sci.* **70,** 3773–3789
12. Pekow, J. R., and Kwon, J. H. (2012) MicroRNAs in inflammatory bowel disease. *Inflamm. Bowel Dis.* **18,** 187–193
13. Sadegh, M. K., Ekman, M., Rippe, C., Uvelius, B., Swärd, K., and Albinsson, S. (2012) Deletion of Dicer in smooth muscle affects voiding pattern and reduces detrusor contractility and neuroeffector transmission. *PLoS One* **7,** e35882
14. Zhang, S., Lv, J. W., Yang, P., Yu, Q., Pang, J., Wang, Z., Guo, H., Liu, S., Hu, J., Li, J., Leng, J., Huang, Y., Ye, Z., and Wang, C. Y. (2012) Loss of dicer exacerbates cyclophosphamide-induced bladder overactivity by enhancing purinergic signaling. *Am. J. Pathol.* **181,** 937–946
15. Ekman, M., Bhattachariya, A., Dahan, D., Uvelius, B., Albinsson, S., and Swärd, K. (2013) Mir-29 repression in bladder outlet obstruction contributes to matrix remodeling and altered stiffness. *PLoS One* **8,** e82308
16. Imamura, M., Sugino, Y., Long, X., Slivano, O. J., Nishikawa, N., Yoshimura, N., and Miano, J. M. (2013) Myocardin and microRNA-1 modulate bladder activity through connexin 43 expression during post-natal development. *J. Cell. Physiol.* **228,** 1819–1826
17. Monastyrskaya, K., Sánchez-Freire, V., Hashemi Gheinani, A., Klumpp, D. J., Babiychuk, E. B., Draeger, A., and Burkhard, F. C. (2013) miR-199a-5p regulates urothelial permeability and may play a role in bladder pain syndrome. *Am. J. Pathol.* **182,** 431–448
18. Klumpp, D. J., Weiser, A. C., Sengupta, S., Forrestal, S. G., Batler, R. A., and Schaeffer, A. J. (2001) Uropathogenic *Escherichia coli* potentiates type 1 pilus-induced apoptosis by suppressing NF-κB. *Infect. Immun.* **69,** 6689–6695
19. Rickard, A., Dorokhov, N., Ryerse, J., Klumpp, D. J., and McHowat, J. (2008) Characterization of tight junction proteins in cultured human urothelial cells. *In Vitro Cell. Dev. Biol. Anim.* **44,** 261–267
20. Earley, S., Heppner, T. J., Nelson, M. T., and Brayden, J. E. (2005) TRPV4 forms a novel Ca^{2+} signaling complex with ryanodine receptors and BKCa channels. *Circ. Res.* **97,** 1270–1279
21. Sánchez Freire, V., Burkhard, F. C., Schmitz, A., Kessler, T. M., and Monastyrskaya, K. (2011) Structural differences between the bladder dome and trigone revealed by mRNA expression analysis of cold-cut biopsies. *BJU Int.* **108,** E126–E135
22. Monastyrskaya, K., Babiychuk, E. B., Hostettler, A., Wood, P., Grewal, T., and Draeger, A. (2009) Plasma membrane-associated annexin A6 reduces Ca^{2+} entry by stabilizing the cortical actin cytoskeleton. *J. Biol. Chem.* **284,** 17227–17242
23. Li, B., and Dewey, C. N. (2011) RSEM: accurate transcript quantification from RNA-Seq data with or without a reference genome. *BMC Bioinformatics* **12,** 323
24. Gentleman, R. C., Carey, V. J., Bates, D. M., Bolstad, B., Dettling, M., Dudoit, S., Ellis, B., Gautier, L., Ge, Y., Gentry, J., Hornik, K., Hothorn, T., Huber, W., Iacus, S., Irizarry, R., Leisch, F., Li, C., Maechler, M., Rossini, A. J., Sawitzki, G., Smith, C., Smyth, G., Tierney, L., Yang, J. Y., and Zhang, J. (2004) Bioconductor: open software development for computational biology and bioinformatics. *Genome Biol.* **5,** R80
25. Kropp, B. P., Zhang, Y., Tomasek, J. J., Cowan, R., Furness, P. D., 3rd, Vaughan, M. B., Parizi, M., and Cheng, E. Y. (1999) Characterization of cultured bladder smooth muscle cells: assessment of *in vitro* contractility. *J. Urol.* **162,** 1779–1784
26. Martin, A. F., Bhatti, S., Pyne-Geithman, G. J., Farjah, M., Manaves, V., Walker, L., Franks, R., Strauch, A. R., and Paul, R. J. (2007) Expression and function of COOH-terminal myosin heavy chain isoforms in mouse smooth muscle. *Am. J. Physiol. Cell Physiol.* **293,** C238–C245
27. Alexander, M. S., Kawahara, G., Motohashi, N., Casar, J. C., Eisenberg, I., Myers, J. A., Gasperini, M. J., Estrella, E. A., Kho, A. T., Mitsuhashi, S., Shapiro, F., Kang, P. B., and Kunkel, L. M. (2013) MicroRNA-199a is induced in dystrophic muscle and affects WNT signaling, cell proliferation, and myogenic differentiation. *Cell Death Differ.* **20,** 1194–1208

28. Ueki, N., Sobue, K., Kanda, K., Hada, T., and Higashino, K. (1987) Expression of high and low molecular weight caldesmons during phenotypic modulation of smooth muscle cells. *Proc. Natl. Acad. Sci. U.S.A.* **84,** 9049–9053
29. Zheng, X. L. (2014) Myocardin and smooth muscle differentiation. *Arch. Biochem. Biophys.* **543,** 48–56
30. Luo, X. G., Zhang, C. L., Zhao, W. W., Liu, Z. P., Liu, L., Mu, A., Guo, S., Wang, N., Zhou, H., and Zhang, T. C. (2014) Histone methyltransferase SMYD3 promotes MRTF-A-mediated transactivation of MYL9 and migration of MCF-7 breast cancer cells. *Cancer Lett.* **344,** 129–137
31. Iwasaki, K., Hayashi, K., Fujioka, T., and Sobue, K. (2008) Rho/Rho-associated kinase signal regulates myogenic differentiation via myocardin-related transcription factor-A/Smad-dependent transcription of the Id3 gene. *J. Biol. Chem.* **283,** 21230–21241
32. Applebaum, M., Ben-Yair, R., and Kalcheim, C. (2014) Segregation of striated and smooth muscle lineages by a Notch-dependent regulatory network. *BMC Biol.* **12,** 53
33. Cowan, C. E., Kohler, E. E., Dugan, T. A., Mirza, M. K., Malik, A. B., and Wary, K. K. (2010) Kruppel-like factor-4 transcriptionally regulates VE-cadherin expression and endothelial barrier function. *Circ. Res.* **107,** 959–966
34. Chan, Y. C., Roy, S., Huang, Y., Khanna, S., and Sen, C. K. (2012) The microRNA miR-199a-5p down-regulation switches on wound angiogenesis by derepressing the v-ets erythroblastosis virus E26 oncogene homolog 1-matrix metalloproteinase-1 pathway. *J. Biol. Chem.* **287,** 41032–41043
35. Rane, S., He, M., Sayed, D., Vashistha, H., Malhotra, A., Sadoshima, J., Vatner, D. E., Vatner, S. F., and Abdellatif, M. (2009) Downregulation of miR-199a derepresses hypoxia-inducible factor-1α and Sirtuin 1 and recapitulates hypoxia preconditioning in cardiac myocytes. *Circ. Res.* **104,** 879–886
36. Song, X. W., Li, Q., Lin, L., Wang, X. C., Li, D. F., Wang, G. K., Ren, A. J., Wang, Y. R., Qin, Y. W., Yuan, W. J., and Jing, Q. (2010) MicroRNAs are dynamically regulated in hypertrophic hearts, and miR-199a is essential for the maintenance of cell size in cardiomyocytes. *J. Cell. Physiol.* **225,** 437–443
37. Cheung, H. H., Davis, A. J., Lee, T. L., Pang, A. L., Nagrani, S., Rennert, O. M., and Chan, W. Y. (2011) Methylation of an intronic region regulates miR-199a in testicular tumor malignancy. *Oncogene* **30,** 3404–3415
38. Bowen, T., Jenkins, R. H., and Fraser, D. J. (2013) MicroRNAs, transforming growth factor β-1, and tissue fibrosis. *J. Pathol.* **229,** 274–285
39. Meng, X. M., Chung, A. C., and Lan, H. Y. (2013) Role of the TGF-β/BMP-7/Smad pathways in renal diseases. *Clin. Sci.* **124,** 243–254
40. Lino Cardenas, C. L., Henaoui, I. S., Courcot, E., Roderburg, C., Cauffiez, C., Aubert, S., Copin, M. C., Wallaert, B., Glowacki, F., Dewaeles, E., Milosevic, J., Maurizio, J., Tedrow, J., Marcet, B., Lo-Guidice, J. M., Kaminski, N., Barbry, P., Luedde, T., Perrais, M., Mari, B., and Pottier, N. (2013) miR-199a-5p Is upregulated during fibrogenic response to tissue injury and mediates TGFβ-induced lung fibroblast activation by targeting caveolin-1. *PLoS Genet.* **9,** e1003291
41. Mendell, J. T., and Olson, E. N. (2012) MicroRNAs in stress signaling and human disease. *Cell* **148,** 1172–1187
42. Shen, Q., Cicinnati, V. R., Zhang, X., Iacob, S., Weber, F., Sotiropoulos, G. C., Radtke, A., Lu, M., Paul, A., Gerken, G., and Beckebaum, S. (2010) Role of microRNA-199a-5p and discoidin domain receptor 1 in human hepatocellular carcinoma invasion. *Mol. Cancer* **9,** 227
43. Hu, Y., Liu, J., Jiang, B., Chen, J., Fu, Z., Bai, F., Jiang, J., and Tang, Z. (2014) MiR-199a-5p loss up-regulated DDR1 aggravated colorectal cancer by activating epithelial-to-mesenchymal transition related signaling. *Dig. Dis. Sci.* **59,** 2163–2172
44. Roncarati, R., Viviani Anselmi, C., Losi, M. A., Papa, L., Cavarretta, E., Da Costa Martins, P., Contaldi, C., Saccani Jotti, G., Franzone, A., Galastri, L., Latronico, M. V., Imbriaco, M., Esposito, G., De Windt, L., Betocchi, S., and Condorelli, G. (2014) Circulating miR-29a, among other up-regulated microRNAs, is the only biomarker for both hypertrophy and fibrosis in patients with hypertrophic cardiomyopathy. *J. Am. Coll. Cardiol.* **63,** 920–927
45. Reya, T., and Clevers, H. (2005) Wnt signalling in stem cells and cancer. *Nature* **434,** 843–850
46. Onizuka, T., Yuasa, S., Kusumoto, D., Shimoji, K., Egashira, T., Ohno, Y., Kageyama, T., Tanaka, T., Hattori, F., Fujita, J., Ieda, M., Kimura, K., Makino, S., Sano, M., Kudo, A., and Fukuda, K. (2012) Wnt2 accelerates cardiac myocyte differentiation from ES-cell derived mesodermal cells via non-canonical pathway. *J. Mol. Cell. Cardiol.* **52,** 650–659
47. Goodwin, A. M., and D'Amore, P. A. (2002) Wnt signaling in the vasculature. *Angiogenesis* **5,** 1–9
48. Goss, A. M., Tian, Y., Cheng, L., Yang, J., Zhou, D., Cohen, E. D., and Morrisey, E. E. (2011) Wnt2 signaling is necessary and sufficient to activate the airway smooth muscle program in the lung by regulating myocardin/Mrtf-B and Fgf10 expression. *Dev. Biol.* **356,** 541–552
49. Wang, H., Gilner, J. B., Bautch, V. L., Wang, D. Z., Wainwright, B. J., Kirby, S. L., and Patterson, C. (2007) Wnt2 coordinates the commitment of mesoderm to hematopoietic, endothelial, and cardiac lineages in embryoid bodies. *J. Biol. Chem.* **282,** 782–791
50. Tsaousi, A., Williams, H., Lyon, C. A., Taylor, V., Swain, A., Johnson, J. L., and George, S. J. (2011) Wnt4/β-catenin signaling induces VSMC proliferation and is associated with intimal thickening. *Circ. Res.* **108,** 427–436
51. Sasaki, T., Hwang, H., Nguyen, C., Kloner, R. A., and Kahn, M. (2013) The small molecule Wnt signaling modulator ICG-001 improves contractile function in chronically infarcted rat myocardium. *PLoS One* **8,** e75010
52. Liu, Y., Sinha, S., McDonald, O. G., Shang, Y., Hoofnagle, M. H., and Owens, G. K. (2005) Kruppel-like factor 4 abrogates myocardin-induced activation of smooth muscle gene expression. *J. Biol. Chem.* **280,** 9719–9727
53. Zhang, X., Azhar, G., Helms, S. A., and Wei, J. Y. (2011) Regulation of cardiac microRNAs by serum response factor. *J. Biomed. Sci.* **18,** 15
54. Lu, T. Y., Lin, B., Li, Y., Arora, A., Han, L., Cui, C., Coronnello, C., Sheng, Y., Benos, P. V., and Yang, L. (2013) Overexpression of microRNA-1 promotes cardiomyocyte commitment from human cardiovascular progenitors via suppressing WNT and FGF signaling pathways. *J. Mol. Cell. Cardiol.* **63,** 146–154
55. Wu, Z. Y., Lu, L., Liang, J., Guo, X. R., Zhang, P. H., and Luo, S. J. (2014) Keloid microRNA expression analysis and the influence of miR-199a-5p on the proliferation of keloid fibroblasts. *Genet. Mol. Res.* **13,** 2727–2738
56. Hsu, C. Y., Hsieh, T. H., Tsai, C. F., Tsai, H. P., Chen, H. S., Chang, Y., Chuang, H. Y., Lee, J. N., Hsu, Y. L., and Tsai, E. M. (2014) miRNA-199a-5p regulates VEGFA in endometrial mesenchymal stem cells and contributes to the pathogenesis of endometriosis. *J. Pathol.* **232,** 330–343
57. Yang, J., Li, X., Li, Y., Southwood, M., Ye, L., Long, L., Al-Lamki, R. S., and Morrell, N. W. (2013) Id proteins are critical downstream effectors of BMP signaling in human pulmonary arterial smooth muscle cells. *Am. J. Physiol. Lung Cell. Mol. Physiol.* **305,** L312–L321
58. Mohamed, J. S., Lopez, M. A., Cox, G. A., and Boriek, A. M. (2013) Ankyrin repeat domain protein 2 and inhibitor of DNA binding 3 cooperatively inhibit myoblast differentiation by physical interaction. *J. Biol. Chem.* **288,** 24560–24568
59. Guo, Y., Xiao, L., Sun, L., and Liu, F. (2012) Wnt/β-catenin signaling: a promising new target for fibrosis diseases. *Physiol. Res.* **61,** 337–346